

**AN APPROACH TO ROLLOVER STABILITY IN VEHICLES USING
SUSPENSION RELATIVE POSITION SENSORS AND LATERAL
ACCELERATION SENSORS**

A Thesis

by

NARAHARI VITTAL RAO

Submitted to the Office of Graduate Studies of
Texas A&M University
in partial fulfillment of the requirements for the degree of
MASTER OF SCIENCE

December 2005

Major Subject: Mechanical Engineering

**AN APPROACH TO ROLLOVER STABILITY IN VEHICLES USING
SUSPENSION RELATIVE POSITION SENSORS AND LATERAL
ACCELERATION SENSORS**

A Thesis

by

NARAHARI VITTAL RAO

Submitted to the Office of Graduate Studies of
Texas A&M University
in partial fulfillment of the requirements of the degree of

MASTER OF SCIENCE

Approved by:

Chair of Committee,	Reza Langari
Committee Members,	Darbha Swaroop
	Shankar Bhattacharyya
Head of Department,	Dennis L. O'Neal

December 2005

Major Subject: Mechanical Engineering

ABSTRACT

An Approach to Rollover Stability in Vehicles Using Suspension Relative Position Sensors and Lateral Acceleration Sensors. (December 2005)

Narahari Vittal Rao,

B.E., Vishveswariah Technological University

Chair of Advisory Committee: Dr. Reza Langari

Safety in automobiles is gaining increasing importance. With the increasing trend of U.S. buyers towards SUVs, appropriate safety measures for SUVs need to be implemented. Since SUVs, as a vehicle type, have a higher center of gravity and hence have a greater tendency to rollover at high cornering speeds. The rollover can also occur due to the vertical road inputs like bumps and potholes which induce a rolling moment.

The proposed rollover identification system would “couple” the two inputs from the suspension relative position sensors and the lateral acceleration sensor to predict rollover. The input to the suspension relative position sensors could be either due to the vehicle cornering, which results in the outer suspension getting compressed and the inner suspension getting extended, or maybe due to vertical road inputs. The principal objective is to differentiate the two types of inputs (since they can have opposing moment values) and further couple the same with the lateral acceleration input to form a rollover identification system.

The work involves modeling of a semi-car model using the Dymola-vehicle dynamics simulation software. The semi-car model is developed to simulate values for the two proposed sensors. Then using NHTSA standard steering procedures and steering angle as the input, the lateral tire forces are generated. These tire forces serve as input to the Dymola model which is integrated into a Simulink model. The lateral acceleration and

suspension relative position sensor values obtained are then used by LabVIEW to pass judgments on the type of rollover.

The model was successfully developed in Dymola. The model with steering angle as input was able to generate values of lateral acceleration and lateral tire forces. The roll angle induced due to road inputs and vehicle cornering were estimated. Since the principal objective of modeling was to generate lateral acceleration values, these values were subsequently used in the LabVIEW Rollover Identification System where rollover induced either by maneuver or through road inputs were clearly identified.

To Amma, Anna,
Usha, Aishu
and
Nethra

ACKNOWLEDGMENTS

It so often happens that people who worked behind the scenes to make things happen seldom get noticed. I guess the foundation of acknowledgements lies in the very idea to eliminate this discrepancy and give due credit to those people who have equally contributed to the endeavor.

First of all, I would like to thank my chair Dr. Reza Langari whose unflinching support and co-operation saw me through this thesis. His patience and very strong emphasis on fundamentals was certainly an inspiration and an attribute to emulate.

Also I would like to thank Dr. Swaroop and Dr. Bhattacharyya, my committee members whose feedback and invaluable time and support were an essential ingredient to the completion of this research.

My mother and my father, whose blessings and encouragement were an invaluable asset in my research. My odyssey without their moral support and love in me would not have been complete.

My supportive sister, my naughty niece Aishu and of course the ever wonderful Nethra, provided the shadow of faith that was so indispensable.

I also would like to extend my warm appreciation to everyone in my research group, my innumerable friends at Texas A&M and to Texas A&M University.

Last but not the least, God whose blessings has always seen me pass through thick and thin with utmost ease. His grace and my devotion in him have seen me face hurdles with a stoic attitude. He is the elixir to all my queries and I owe all that I have to him.

TABLE OF CONTENTS

	Page
ABSTRACT	iii
DEDICATION	v
ACKNOWLEDGMENTS.....	vi
TABLE OF CONTENTS	vii
LIST OF FIGURES.....	ix
LIST OF TABLES	xi
CHAPTER	
I INTRODUCTION	1
1.1 Overview.....	1
1.2 Defining Rollover	2
1.3 Objectives and Problem Definition.....	4
1.4 Methodology	7
II LITERATURE SURVEY.....	9
2.1 Introduction.....	9
2.2 Rollover Statistics	11
2.3 Vehicle Models	12
2.4 Rollover Identification	13
2.5 Rollover Control and Prevention	15
III VEHICLE MODELING.....	17
3.1 Overview of Dymola.....	17
3.2 Semi-Car Model.....	18
3.3 Dymola Model	20
3.3.1 Lateral Tire Force Determination	22
3.3.2 Relation between Tire Forces and Steering Angle	23
3.3.3 Steering Profile	25
3.3.4 Determination of Cornering Stiffness.....	32
3.3.5 Predictive Modeling.....	34
3.3.6 Simulink Model	35

CHAPTER	Page
IV ROLLOVER IDENTIFICATION SYSTEM	39
4.1 Software Integration.....	39
4.2 Reasons for Choosing LabVIEW.....	41
4.3 Rollover Identification System	41
V RESULTS AND DISCUSSIONS.....	47
5.1 Dymola and Simulink Models	47
5.2 Rollover Identification System	53
VI SUMMARY AND FUTURE WORK	58
REFERENCES.....	59
APPENDIX I- NOMENCLATURE.....	62
APPENDIX II- MATLAB CODE FOR CALCULATION OF LATERAL TIRE FORCES USING STEERING PROFILE AS THE INPUT.....	64
APPENDIX III- VEHICLE PARAMETERS USED FOR STUDY.....	84
APPENDIX IV- DERIVATION OF ROLL ANGLE DETERMINATION FOR SUSPENSION RELATIVE POSITION SENSOR MEASUREMENT.....	85
VITA.....	88

LIST OF FIGURES

FIGURE	Page
1 Graphical description of forces that induce rollover in vehicle	4
2 Vehicle body roll and suspension deflections during a) a right turn on smooth road b) driving straight on uneven road	5
3 Illustration indicating SSF in cars and higher C.G like vehicles	10
4 Trends in SSF a) by SUV Type b) by vehicle type and model year ...	10
5 An example of robot model created in Dymola	18
6 Semi-car rollover model.....	19
7 Semi-car rollover model developed in Dymola	21
8 Screen shot of the Dymola model and the software interface.....	22
9 Schematic representation of Dymola model as a black box	23
10 Mathematical model depicting the relation between the vehicle speed, yaw rate and the slip angle.....	24
11 NHTSA fishhook 1A maneuver description.....	27
12 Fishhook 1A maneuver in Matlab	29
13 Graphical representation of fishhook maneuver	29
14 Lateral force variation for different sections of the steering profile...	31
15 Lateral force vs. slip angle for a racing tire	32
16 Dependency of cornering stiffness on slip angle for entry speed of 50 kmph.....	33
17 Lateral front tire forces for the given steering profile	34
18 Regression plot of roll angle and lateral acceleration.....	35
19 Simulink model connecting Dymola and the Matlab code to generate lateral acceleration values as the output	38
20 Data flow within the software integration	40
21 Front panel of the rollover identification system.....	42
22 Rollover identification system reading input files from Simulink	43
23 Peak detector and property node.....	43
24 Yaw rate of the vehicle	48
25 Steering angle vs. time.....	48

FIGURE	Page
26 Variation of lateral tire force (N) vs. time	49
27 Variation of lateral acceleration vs. time	50
28 Relative suspension movement vs. time	50
29 Linear regression line plotted for roll angle and lateral acceleration .	51
30 Plot of original roll angle (without the uncorrected roll center height and lateral shift in C.G) and corrected roll angle.....	52
31 Anova analysis on roll angle data	52
32 LTR for the Dymola model	53
33 Front panel indicators for case 1	54
34 Front panel indicators for case 2.....	55
35 Front panel indicators for case 3.....	56
36 Front panel indicators for case 4.....	56

LIST OF TABLES

TABLE		Page
1	Matrix demonstrating the sensors and their measurement parameter	6
2	Vehicle parameters and their associated values.....	20
3	Summary of rollover resistance maneuver scores	26
4	Variation of hand wheel steering angle with respect to time.....	28
5	Variation of yaw rates for the front tires with steering profile	31
6	Summary table for determining presence of suspension deflection or variation of lateral acceleration	45

CHAPTER I

INTRODUCTION

1.1 Overview

Over the years there has been a considerable increase in the dependence on automobiles and subsequently this has led to a spurt in automotive sales. In the U.S alone, 87.9% of everyday commuters use private vehicles for commutation. With most Americans living in low-density communities, public transportation is neither viable nor profitable. Honda Automotive alone reported an increase of 2.4 % [1] in their North America sales while German automaker BMW reported 8.6% rise in sales as compared to the previous year. With the number of cars continuously increasing so are the numbers of accidents. According to the National Highway Traffic Safety Administration (NHTSA) preliminary projected report for 2004 [2], there is an increase of 0.5% in the number of people killed in 2004 as compared to 2003 and also accompanied by a 0.1% increase in the number of fatal crashes. SUVs as a vehicle type contributes most to occupants killed in vehicle crashes. As compared to 2003, 2004 saw a sudden upsurge of 4.9 % fatality rate for SUV occupants while large trucks saw an increase of 6.2% in the number of occupants killed in vehicle crash. This certainly is a cause for concern.

SUVs and pickup trucks generally ride higher off the ground than passenger cars and have higher centers of gravity (CG), which make them more prone to rolling over. Rollover crashes are one of the most crucial safety concerns for all classes of light vehicles especially light truck vehicles ~LTV's (pickups, sport utility vehicles, and vans). In terms of fatalities per registered vehicle, rollovers are second only to frontal crashes in their level of severity. The rollover problem is more serious for light trucks, especially sport utility vehicles. For all types of collisions, LTV's are only in 68 percent

This thesis follows the style and format of ASME Journal of Dynamic Systems, Measurement, and Control.

as many crashes per registered vehicle as are passenger cars. However, for rollover crashes, LTV's are as high as 127 percent as many crashes per registered vehicle as are passenger cars [3].

On-road un-tripped rollovers due to vehicle maneuvering constitute only a small portion of the rollover safety problem. NHTSA's past research has estimated that less than 10 percent of all rollovers are on-road, un-tripped, events. Even though this is a small part of the overall rollover crash problem, considerable attention is given to this problem by proponents of rollover safety [3].

In comparison with tripped, off-road rollover, the causes of un-tripped, on-road rollover are not very well understood. Past NHTSA research has never found a light vehicle for which, when empty, the most severe attainable steady state turn exceeds the vehicle's rollover threshold [3].

The very basic objective of the above statistics is to highlight the importance of a requirement for rollover stability control in automobiles mainly SUVs. With the increasing trend of American car buyers towards SUVs, rollover identification and more importantly rollover prevention becomes very crucial. There are several active chassis control systems that which can influence the vehicle dynamics like by changing the yaw angle hence changing the vehicle course or by deploying safety systems like SRS seat belts and air bags. But it is very essential to develop a system that which can identify a rollover.

1.2 Defining Rollover

Rollover is defined as “any maneuver in which the vehicle rotates 90^0 or more about its longitudinal axis such that the body makes contact with the ground. [4]” In plain terms, when the vehicle has a high center of gravity or the curvature of the road is such that the

resistance offered by the shift in weight of tires is less than the outward cornering force then the vehicle rolls over. SUVs and pickup trucks generally ride higher off the ground than passenger cars and have higher centers of gravity (CG), which make them more prone to rolling over.

The principal factors that influence rollover stability in automobiles are as described below: [4]

1. The lateral acceleration in the vehicle is far greater than the force provided by the lateral shift in the weight of the tires.
2. The inclination of the ground on which the vehicle is traveling.
3. Obstacles on the road such as bumps, soft ground etc.
4. High center of gravity of heavy vehicles under loaded condition.
5. The radius of curvature of the road on which the vehicle is cornering.
6. Variation in the suspension stiffness of the inner and outer wheels.
7. Driver reaction and input to the system.

Rollover Identification is currently achieved through several means like using a simple system comprising of a single axis accelerometer, a solid-state rate gyro and a micro-controller [5]. Sensors such as these are instrumental in measuring absolute lateral acceleration and roll angle. Using data obtained from these sensors, predictive algorithms can predict impending rollovers by forecasting data. But it is very essential to note that these sensors predict rollover which is maneuver induced and not due to vertical road inputs.

For rollover detection, it is very advantageous to know both the roll angle and the roll rate of the vehicle. The synergy of the lateral acceleration sensor, vertical acceleration sensor, roll rate sensor and longitudinal acceleration sensor are able to estimate roll angles but are not accurate for angles $5-20^{\circ}$ [6]. And this approach is not good when

rollover is induced partially by road inputs. Vehicle roll is primarily caused by body inertial forces and the inputs from uneven road. Each one of these inputs acting alone is sufficient enough to rollover the vehicle. The above mentioned sensor set is capable of measuring roll angles induced primarily by maneuver inputs. This is illustrated in Figure 1 below.

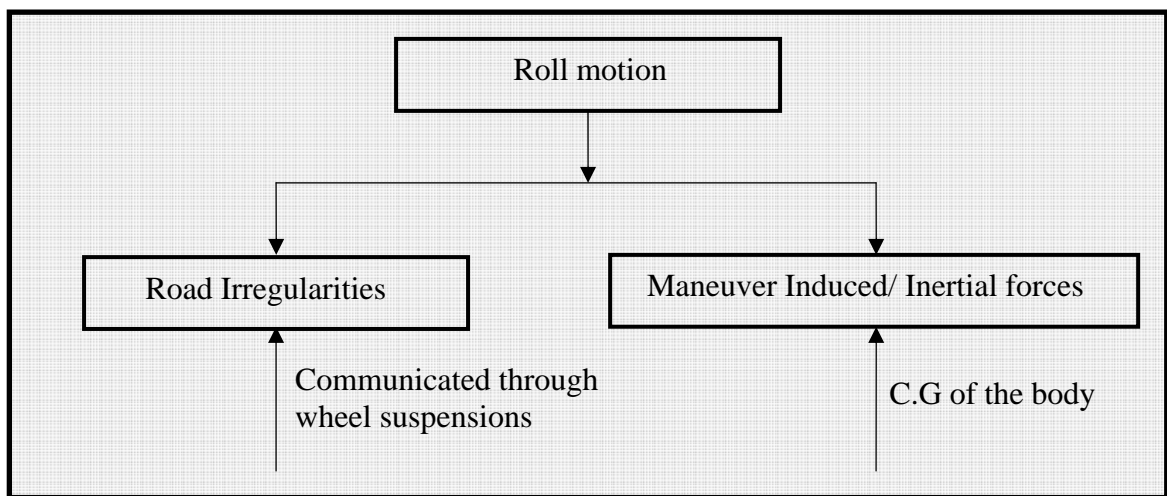


Fig. 1 Graphical description of forces that induce rollover in vehicle

1.3 Objectives and Problem Definition

It is desired to combine two sensor sets in order to predict roll angles and roll rate in vehicles. The two sensor sets are suspension relative position sensors and the lateral acceleration sensor. The suspension relative position sensors are mounted on the front two suspensions and measure the relative movement between the two suspensions. As the vehicle corners, the outer suspension compress while the inner suspension extends. Using a simple dynamic equation the roll angle can be estimated. But clear distinction

needs to be made for suspension deflection due to cornering and deflection due to vehicle road inputs.

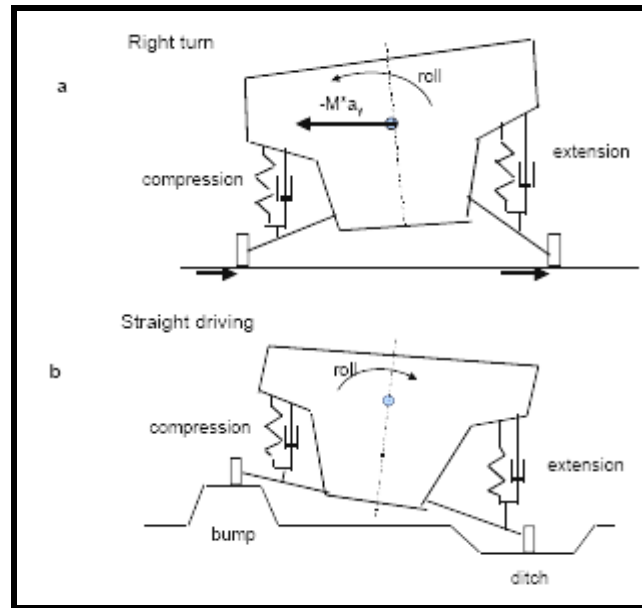


Fig. 2 Vehicle body roll and suspension deflections during a) a right turn on smooth road, b) driving straight on uneven road [6]

Illustrating using an example given in *Hac et al* [6], consider a car making a right turn as shown in Figure 2. The inertial force acts to the left thus shifting the C.G of the vehicle to the left and creating an anti-clockwise moment. This results in the outer suspension getting compressed and the inner suspension gets extended. But if the vehicle were to be going in a straight line and the left wheel comes in contact with a bump while the left wheel simultaneously goes over a pothole, similar suspension deflections are obtained as in the case of vehicle cornering with the outer suspension getting compressed and the inner suspension getting extended. But the moment that is acting on the vehicle is clockwise, opposite in sign as compared to the vehicle cornering case and the vehicle would rollover in the opposite direction than predicted. Therefore distinction needs to be made between suspension deflection that is obtained via road inputs and vehicle cornering.

It is to be noted that during straight line travel of the vehicle even though there could be suspension deflection due to road inputs, if the lateral acceleration is measured at that point, then there would be no change in the measured lateral velocity. The lateral acceleration only results when the vehicle corners. Hence using the lateral acceleration input the distinction between the suspension deflections, obtained through vehicle cornering or by vertical road inputs, could be made.

The matrix below in Table 1 shows the inputs that can cause rollover in vehicles and the corresponding sensors which can measure them. Our approach here is to couple the inputs from both the sensors so that we could predict rollover in all cases.

Table 1 Matrix demonstrating the sensors and their measurement parameter

	Relative Position sensor	Lateral Acceleration Sensor	Comments
Road Inputs	✓	✗	<i>Identify this feedback as road inputs would not induce change in lateral velocity</i>
Cornering Forces	✗	✓	<i>Only the lateral acceleration sensor is excited</i>
Road Inputs+ Cornering Forces	✓	✓	<i>Couple the output from both the sensors to form a system that can predict rollover either due to road inputs or due to cornering forces</i>

1.4 Methodology

Firstly, a threshold limit for the relative value of the suspension movement is set. This could be done considering the maximum suspension deflection possible for that pair of suspensions, by determining the maximum size of the potholes and bumps that could be encountered and also by measuring the maximum allowable shift in the C.G of the vehicle. Since suspension deflection could be either due to vehicle cornering or due to vertical road inputs, the lateral acceleration is measured. If the value of the lateral velocity rate is changing with respect to time, then it can be inferred that the suspension deflection is due to the cornering forces acting on the vehicle.

Using Equation (1) given in Hac [6], the roll angle is estimated. The derivation of the same is shown in Appendix IV.

$$\phi_{erp} = \frac{(\Delta z_{LF} - \Delta z_{RF} + \Delta z_{LR} - \Delta z_{RR})}{2 \cdot t_w} - \frac{M \cdot a_{ym} \cdot h}{k_{tireroll}} \quad (1)$$

Supposing if the suspension deflection is measured but there is no appreciable change in the lateral velocity rate then the vehicle is not cornering and that the deflection is due to the vertical road inputs only. The roll angle is measured using Equation 2 [6].

$$I_{xxl} \cdot d^2 \phi / dt^2 + c_{roll} \cdot d\phi / dt + k_{roll} \cdot \phi = -M_s \cdot a_{ym} \cdot h_{roll} \quad (2)$$

A case may arise when the set threshold value in the suspension deflection has not been reached yet the value of the lateral acceleration is very high. Hence it is ensured that along with the suspension deflection measurement, the lateral acceleration values and/ or $\dot{\phi}$ is constantly being measured. If the value for these parameters exceeds the set threshold limit, then rollover control is initiated irrespective of the suspension deflection measurements.

The suspension deflection measurements is primarily measured since this input can be dichotomous i.e. it can result either due to vehicle cornering or due to vertical road inputs. To eliminate the ambiguity the suspension deflection measurements are measured first. Once the difference between the suspension deflection due to vertical road inputs and vehicle cornering is established, then the lateral acceleration is measured to verify if it is high enough for initiation of active rollover control. But the lateral acceleration is always constantly monitored since they are devoid of any ambiguity.

Once such an algorithm is developed, it needs to be implemented on an actual vehicle by suitably interfacing with an active chassis control system. The algorithm would be instrumental in predicting rollover but to prevent rollover interfacing with an active chassis control system is essential. The algorithm developed in LabVIEW is able to make the judgments about changes in lateral velocity and is also able to perform peak detection for very high lateral acceleration values. Hence the system is capable of recognizing rapid lateral acceleration changes. The system is further tested for different driving conditions and also for its capability of predicting rollover under conditions of maneuver induced rollover and road inputs induced rollover.

CHAPTER II

LITERATURE SURVEY

2.1 Introduction

For over thirty years the problem of rollover in vehicles always has persisted. The National Highway Traffic Safety Administration (NHTSA) in 1973 issued an advanced notice of proposed rulemaking on a rollover resistance standard. The essential objective of this directive was to set up a minimal safety standard for automobiles, in particular SUVs. But the NHTSA due to several problems including some political were unable to formulate a stiff safety standard for Rollover Safety in automobiles. In 1994, NHTSA issued a directive that it had abandoned efforts to develop a rollover standard and instead it focused on developing consumer safety information about vehicle stability.

The static stability factor (SSF) has long been used to describe rollover propensity in automobiles. The Static Stability Factor is defined by the following relation,

$$SSF = \frac{t}{2 \cdot h} \quad (3)$$

where t is the track width and h is the height of the C.G of the car.

SSF rating essentially describes how top-heavy a vehicle is. The higher the value of the SSF, the greater is the safety of the vehicle and less is its chance of rolling over. Most passenger cars have a safety rating of 1.30-1.50 while higher C.G vehicles like SUVs, pick-up trucks and vans have a SSF rating of 1.00-1.30. Below in Figure 3 is an illustration about the description of SSF in cars and higher C.G vehicles.

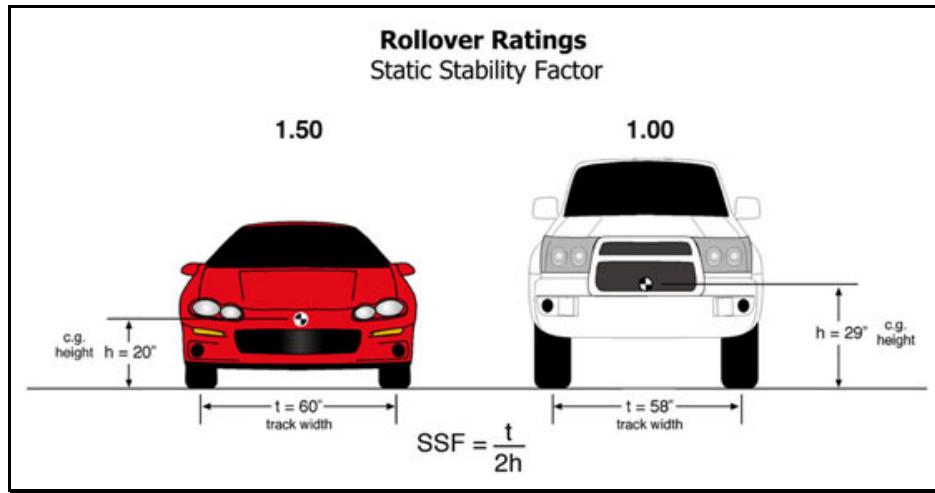


Fig. 3 Illustration indicating SSF in cars and higher C.G vehicles like trucks

Image Courtesy: NHTSA

In Figure 4, the trends in SSF have been plotted both with the type of the vehicle and also the year in which the model was released. It can be observed in Figure 4(a) that since the 90's the trend in SSF for SUVs has always been on the rise. Similarly with all other vehicle types the trend in SSF has always been on the increase.

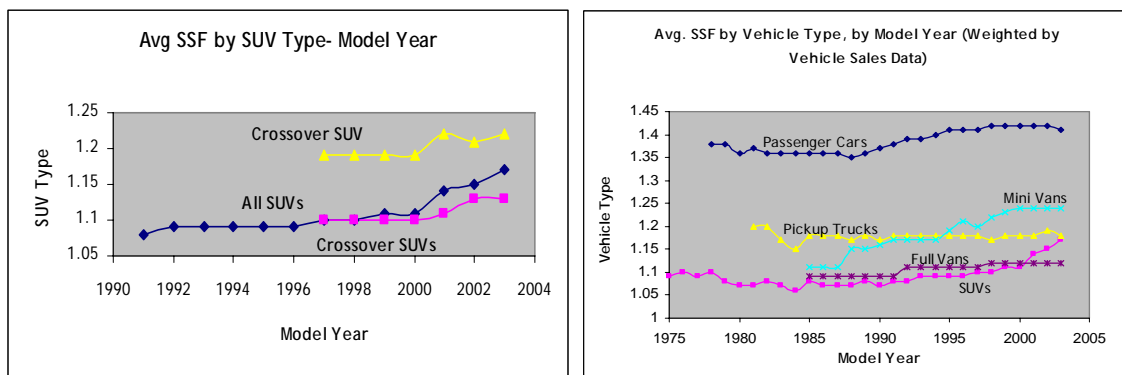


Fig. 4 Trends in SSF a) by SUV type b) by vehicle type and model year

But the SSF cannot be principally used as a distinguishing parameter as it overlooks the vehicle dynamics, the suspension and chassis characteristics and the vehicle and the tire is assumed to be a rigid body. However SSF is an excellent indication to the “rollover propensity” but never an actual measure.

2.2 Rollover Statistics

One in every four new vehicles sold in America today is an SUV. In fact according to a NHTSA report in 2001, 50% of all vehicles sold in US were SUVs, light trucks or vans. Indeed, SUVs are increasingly becoming very popular vehicles among automobile users -- and also the more profitable. Some manufacturers make up to \$15,000 in profits on every SUV that rolls off their assembly line. The sport utility vehicle is one of Detroit's greatest success stories, credited with saving the U.S. auto industry.

With the release of the National Highway Traffic Safety Administration (NHTSA) preliminary report for the year 2004 [2], the statistics shows that there is an increase of 0.5% in the number of people killed in 2004 as compared to 2003 and accompanied by a 0.1% increase in the number of fatal crashes. SUVs as a vehicle type contributed most to occupants killed in vehicle crashes. As compared to 2003, 2004 saw a sudden upsurge of 4.9% fatality rate for SUV occupants with SUVs again registering a 6.9% increase in the passenger vehicle occupants killed and injured in rollover crashes. Early indications for the year 2004 NHTSA report demonstrate that passenger vehicle fatalities for vehicle rollover accidents have increased by 1.1%. Though rollovers are not the frequent type among accident types but they certainly are becoming the more serious type with respect to fatalities.

The above statistics highlight the importance of a requirement for rollover stability identification and subsequently its control in automobiles mainly SUVs. With the

increasing trend of American car buyers towards SUVs, rollover identification and subsequently rollover prevention becomes very crucial.

2.3 Vehicle Models

In order to predict the dynamic behavior of the vehicle, it is very essential to develop a vehicle model which simulates vehicle behavior. Gillespie [4] developed a simple model analyzing the various forces acting on the vehicle. The model assumed a rigid vehicle with a rigid axle. The various forces that were acting on the vehicle were included and a very rough estimate for the lateral acceleration was derived. Later on Gillespie derives a formulation for the quasi-static rollover of a suspended vehicle. In his models he does not take into account the varying front and rear suspension stiffnesses and the tire dynamics. However the formulations give an excellent insight into the dynamics of rollover in vehicles. Most authors who have done work on rollover prediction and stability analysis have developed quarter and semi-car models for their analysis and simulations. Hegazy et al. [7] developed a 94 degree of freedom non-linear multi-body dynamic model of a vehicle. This model is further is used to predict the lateral acceleration, roll angle, roll center height variation, vertical and lateral tire forces and slip angles for a double lane change maneuver. The bicycle model is more commonly used by vehicle dynamics researchers as the one-half of the vehicle is quite as representative of the other half and understanding the dynamics of one side reduces the complexity as well as the computational power. Venhovens et al. [8] tried to model an actual vehicle with as many less assumptions as possible. He was of the view that not all states in the system are observable and it is quite unrealistic to assume that they can be easily measured. He therefore used Kalman filters to estimate some of the parameters. These Kalman filters served as virtual sensors to estimate the vehicle's yaw rate and lateral acceleration in particular areas of operation. He derived a mathematical relation using his bicycle model to establish a relation between the various other vehicle

parameters thus reducing the cost of additional sensors. Huang et al. [9] used a nonlinear active suspension in their half car model to bring about a balance between the ride quality and the suspension travel. The half-car suspension is essentially a linear four degree-of-freedom system consisting of sprung and unsprung masses and tires and suspension systems modeled as a spring mass damper system.

2.4 Rollover Identification

Several methods have been employed to identify and instruct the driver of an impending rollover. External warnings like road signs, warning and caution boards at places where terminally rollover could occur have been implemented. But it is also essential to develop methodologies which would predict a rollover situation according to the type of the vehicle. The vehicle's center of gravity, speed, sprung and unsprung masses and also the suspension dynamics play a crucial role in determining the rollover propensity of a vehicle.

In order to predict the behavior of the vehicle parameters in a dynamic condition, sensors form the "eye" through which the engineer can visualize as to what is happening in the vehicle. A patented predictive rollover sensor was developed by Greene et al. [5] which composed of an array of sensors to measure the different parameters that could cause rollover. The predictive rollover sensor consisted of an accelerometer, solid-state gyro serving as an angular rate sensor and a micro-controller. This sensor combination along with proprietary algorithms claimed to predict rollover. A typical rollover sensing module should ideally be able to detect angular rate of the vehicle, low and high g-forces and also the vertical acceleration. Not only detection is important for rollover but also advanced warning is crucial. The present day electronics fills the vacuum. The electronic sensors chosen should be such that they should not be subjected to forces of gravity. This is because on a banked road or for a vehicle that is subjected to linear accelerations,

angular sensors that are not gravity corrected would be erroneous. For better angular resolution, Schubert et al. [10] says that the accelerometers used should be low-g. It is the combination of these sensors that would predict a rollover condition and hence arm an active/ passive restraint system.

A lot of work has been done in order to predict exact rollover occurrence. Not only the causes of rollover have been understood but also the influence of various chassis components has been studied. Hac [11] tried to analyze the sustained body oscillations that are experienced during an emergency road edge recovery maneuver like a J- turn maneuver. The author infers that the sustained oscillations are primarily due to the coupling that exists between vehicle roll motions, heave and subsequently yaw modes resulting from suspension jacking forces. Hac et al. [6] showed that there is no one sensor that can measure all types of rollover. Since rollover is induced both by maneuver and road inputs, at least combination of two sensors is required to detect rollover stability. A simple lateral acceleration sensor senses lateral acceleration induced through cornering but it fails to take into account the unevenness of the road. While a suspension relative position sensor takes into account the road inputs but fails to predict roll angles for rollover phase. The author goes on to say that the combination of the above two sensors is the best possible approach but the author deviates from developing such a system as their purpose is to develop a stand alone system.

Hac et al. [6] used an observer based approach to model rollover induced both by inertial forces and road inputs. He uses an adaptive closed loop roll observer to estimate roll angles. Since most of the variables are transient and would hence vary with time, these values were compared with the measured outputs and the difference with a suitable gain matrix was fed back into the observer. The choice of the gain matrix lay with the designer. Hac also used two sets of equations to model rollover of the vehicle for before lift-off conditions and after lift-off conditions. Hence the estimation strategy used by

Hac consisted of obtaining the preliminary estimates by processing the sensor inputs and comparing it with the estimates and the second stage of refinement using an observer.

2.5 Rollover Control and Prevention

If rollover identification is the first step then the equally important step of rollover prevention needs to be implemented. There are several active chassis control systems that which can influence the vehicle dynamics like by changing the yaw angle hence changing the vehicle course or by deploying safety systems like SRS seat belts and air bags and thus help to minimize the chances of a rollover. Hac et al. [12] developed several methods for improving vehicle stability and emergency handling by employing actively controlled chassis systems. The vehicle stability can be disturbed by giving sudden inputs to the system as stepping on a throttle or swerving very tightly. Sudden braking or rapid deceleration can lead to locking of the wheels or applying large throttle inputs may result in excessive wheel spin or steering ability loss. During cornering, the yaw angle remains proportional to the steering input for the linear range of tires operation. Sudden inputs could result in changing the vehicle behavior and reaching the non-linear range of operation. Therefore, for most drivers, in order to tide over such a situation active chassis control is used. Active chassis systems may be in the form of active front/ rear wheel steer, active brake control or active roll moment distribution between front and rear via controllable suspensions. These would bring about change in vehicle dynamics like altering the yaw angle which turn would apply a stabilizing moment on the vehicle. The Vehicle Dynamics Control (VDC) system developed by Bosch consists of an array of sensors to measure brake pressure, lateral acceleration, yaw rate, steering angle and wheel speed. VDC acts independent of the driver's input and monitors the system parameters. According to Bosch, this system is capable of reducing jackknifing and rollovers. Odenthal et al. [13] used three feedback loops i.e. continuous operation steering control loop, emergency steering control loop and emergency braking control loop to avoid rollover of vehicles. Ackermann et al. [14] suggested an approach

to rollover avoidance using active steering in which an actuator is used to set a small auxiliary front wheel steering angle in addition to the steering angle input by the driver. The objective was to reduce the risk of transient roll overshoot of the vehicle's body during lane change maneuvers. A new kinetic energy based measure was introduced by Johansson and Gafvert [15] in which a gain scheduled linear quadratic (LQ) controller is used to prevent wheel lift-off. The controller based on a new convex optimization strategy outputs the desired changes of the forces acting on the chassis to the braking and traction system which in turn is commanded by the control allocator. The Johansson and Gafvert model is primarily inspired by the energy considerations during rollover.

Vehicles with higher C.G are more prone to rollover than any other vehicles because of the overturning moment that is created during lane changes or exiting ramps. Lewis et al. [16] primarily developed a nonlinear model for the tractor/semi-trailer. Using lateral acceleration measured at the trailer center of gravity, a control law was developed. A sliding mode robust controller was designed, incorporating the uncertainties in determination of certain properties like the tire cornering stiffness etc., which improved the dynamic performance and roll stability of the vehicle.

CHAPTER III

VEHICLE MODELING

3.1 Overview of Dymola

Dynamic **M**odeling **L**aboratory or Dymola software can be used to model and simulate complex integrated systems. Dymola has in itself a number of built-in libraries for simulation of several components for thermal, fluid, vehicle dynamics, power train and thermodynamic applications. Dymola essentially lets one use an engineering component in visual form which otherwise is needed to be described by differential algebraic equations (DAE).

Dymola is built in such a way that the components can be actually connected as it would otherwise be in the real world. The components would be connected by the means of graphical connections which can be assigned physical properties of couplings like in the real world. The same model can be re-used with different parameters to study different cases. One of the most important aspects about Dymola is that it links with other software like Matlab/ Simulink in an effortless way. This makes the integration of software much easier. One such approach was used in this research to link the Dymola model to Matlab/ Simulink. The Figure 5 below shows one such robot model developed within Dymola.

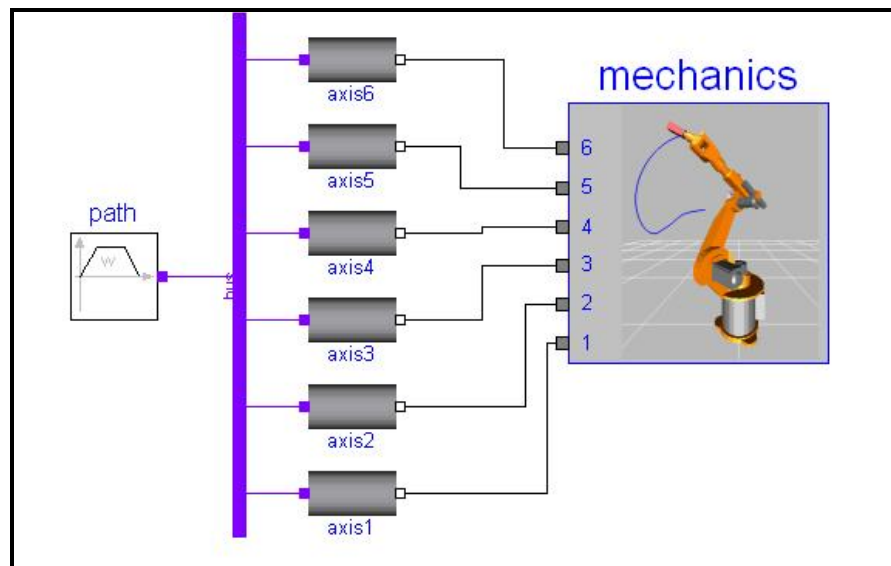


Fig. 5 An example of robot model created in Dymola

3.2 Semi- Car Model

A semi-car model was developed using **Dynamic Modeling Laboratory (Dymola)** to model the dynamics of a car during rollover.

Since the car is symmetric along its longitudinal x-axis, the lateral y-axis and the vertical z-axis, the roll, pitch and yaw motions in order can be studied by analyzing only half or quarter of the car model. A semi-car model is generally used when angular rate of that motion needs to be measured.

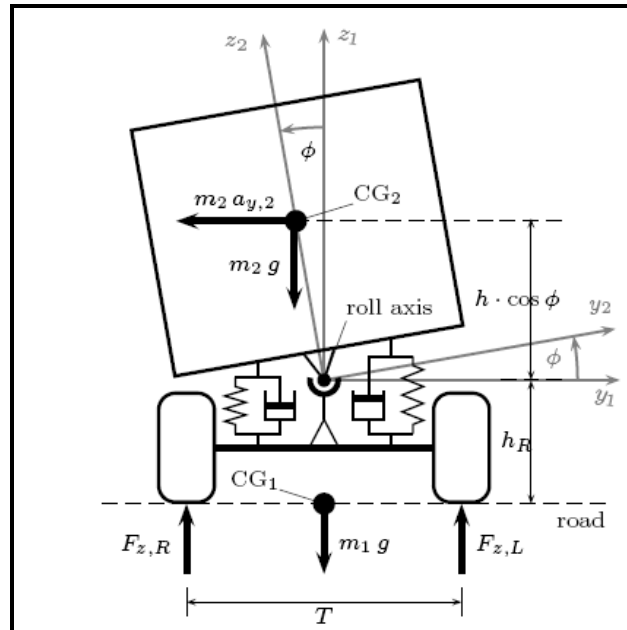


Fig. 6 Semi-car rollover model [17]

In Figure 6, a rollover semi-car model is shown. This car model is adopted from Ackermann et al. [17] paper on damping of roll dynamics by gain scheduled active steering. The semi-car model consists of two masses, the sprung mass that includes the vehicle mass above the suspension system and the unsprung mass which includes the tires, brake systems and other chassis components. The model is assumed to have a fixed roll axis and the roll plane is parallel to the road plane along the longitudinal direction of the vehicle and is at a height, h_R . The suspension system modeled as a linear spring-damper system and the tires modeled as linear springs. The tires are assumed to be in their linear operation.

The values for the each of the individual vehicle components are derived from Kiencke [18] and are as outlined in Table 2.

Table 2 Vehicle parameters and their associated values

<i>Sprung Mass</i>	$m_{sprung} = 350 \text{ kg}$
<i>Unsprung Mass</i>	$m_{unsprung} = 31 \text{ kg}$
<i>Damping constant of the Spring</i>	$c_{damping} = 1140 \text{ N/m/s}$
<i>Stiffness of the suspension system</i>	$k_{suspension} = 20\,900 \text{ N/m}$
<i>Stiffness of tire</i>	$k_{tires} = 10\,800 \text{ N/m}$

3.3 Dymola Model

The semi-car model developed in Dymola is as shown in Figure 7 and the screen shot of the model and the software interface is shown in Figure 8. It is very important to note that the various forces that are acting on the vehicle are referenced with respect to the Earth-fixed axes.

It consists of two sets of springs with spring stiffnesses $S1$ and $S2$ representing the tires. Above this suspension are the unsprung masses $M2$ and $M3$. The spring-damper system $SD1$ and $SD2$ represents the suspension system. Each suspension system has a relative state position sensor ($PS1$ and $PS2$) attached to both its end terminals. $SlidingMass1$ and $SlidingMass2$ represent the sprung mass of the system. The lateral acceleration sensor and the suspension relative position sensor are plugged into the model using the sensors toolbox available within the software. The acceleration sensor is mounted on the sprung mass of the system.

$Force1$ and $Force2$ represent the lateral force at the wheels offered by the ground during right hand cornering. Also the tires are anchored to the ground and prior to lift-off

condition are considered. $Wheel_force_O$ and $Wheel_force_I$ represent the vertical forces acting on the tires.

The unsprung masses $M2$ and $M3$ are taken to be 31 kg each while the sprung mass is taken to be 350 kg (without the passengers). The suspension stiffness is 20900 N/m while the damper co-efficient is 1140 N-s/m in accordance with Table 2. The tire stiffness is 10800 N/m.

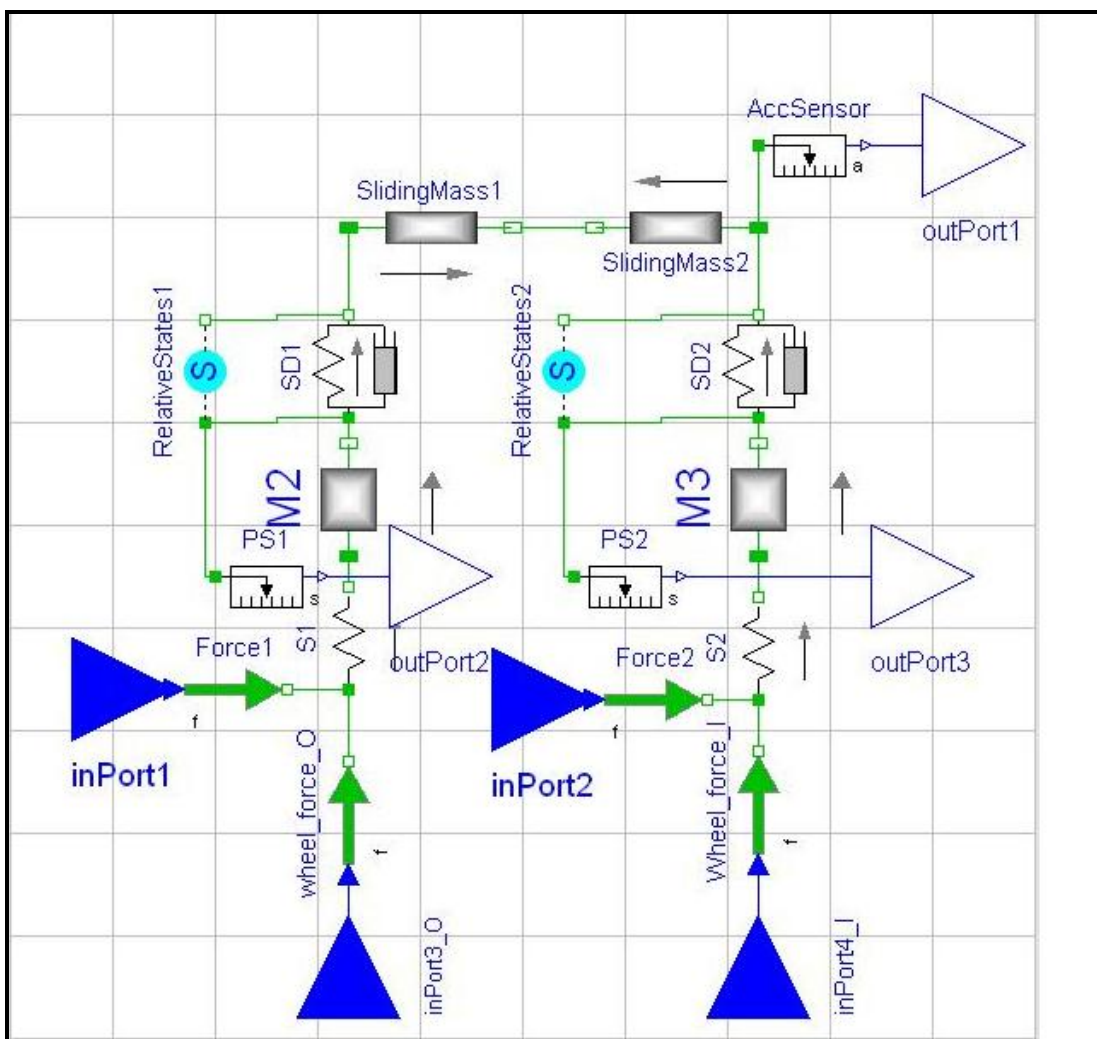


Fig. 7 Semi-car rollover model developed in Dymola

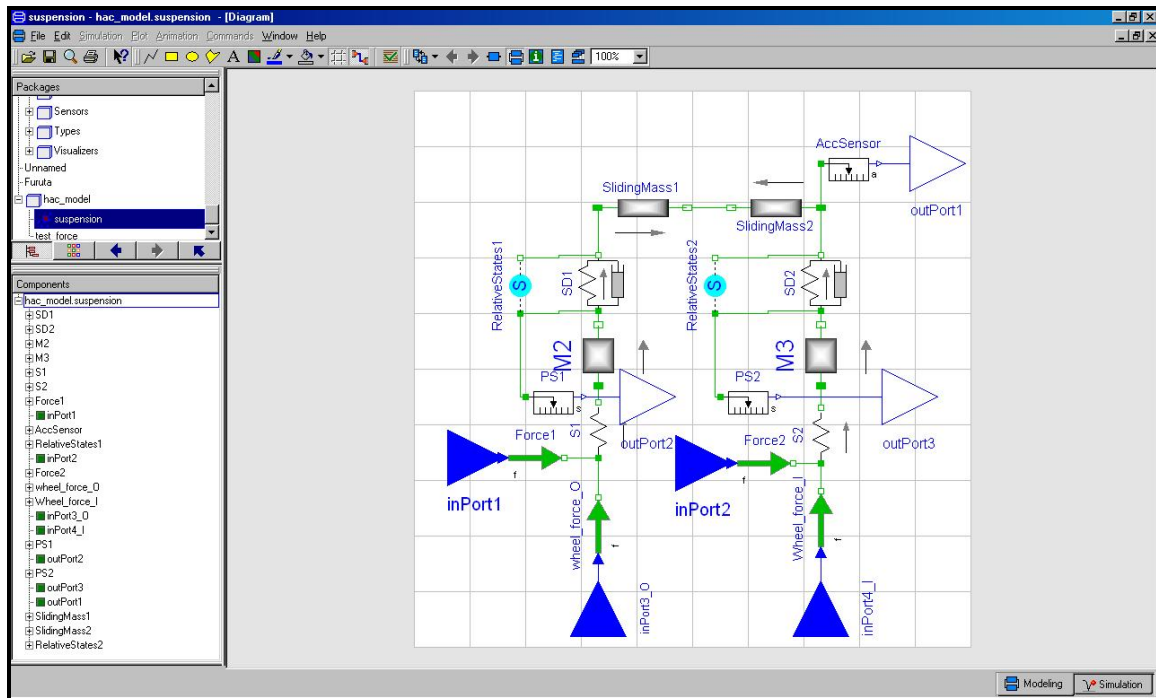


Fig. 8 Screen shot of the Dymola model and the software interface

3.3.1 Lateral Tire Force Determination

It was desired that for the Dymola Model, the steering angle be the input and the lateral acceleration as the output. In order to input the steering angle as a varying parameter, the relation between the steering angle and the lateral tire force needed to be established. The lateral tire forces thus generated from the relation would be used to input into *inport1* and *inport2* on the Dymola model. A schematic representation of the Dymola model as a black box is shown in Figure 9.

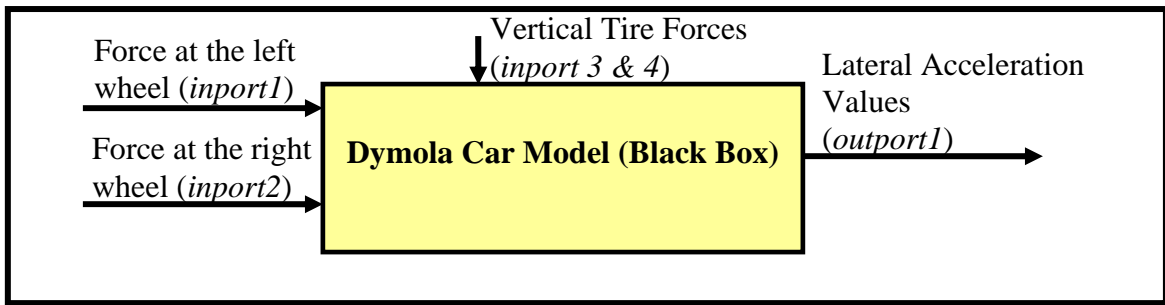


Fig. 9 Schematic representation of Dymola model as a black box

The entire system can be likened to a black-box with 2 inputs for the lateral front tire forces and one output for the lateral acceleration sensor.

3.3.2 Relation between Tire Forces and Steering Angle

Therefore in order to generate the lateral tire forces which would serve as input to the Dymola model, a relation is established with the steering angle. With the steering angle as the input to the system, the lateral tire forces are calculated in a Matlab M-file.

The lateral tire force at the front tire is related to the steering angle by the following relation [14]:

$$F_{y1} = -2 \cdot C_{F\alpha 1} \cdot \alpha_1 \quad (4)$$

Where $C_{F\alpha 1}$ is the Steady state cornering stiffness (N/rad) and α_1 - Front tire slip angle (rad).

The slip angle α_1 is defined by

$$\alpha_1 = \frac{v + a \cdot r}{U} - \frac{\delta}{i_{st}} \quad (5)$$

Where v is the lateral slip velocity (m/s), a = distance of C.G to the front axle (m), r is the yaw rate (rad/s), U = forward vehicle speed (m/s), δ = steering angle (rad) and i_{st} = steering gear ratio.

In (13) for the determination of slip angle, the lateral slip velocity and the yaw rate are the only two unknown parameters.

Most Kalman filters can be assumed to be virtual sensors as unknown states can be estimated from the known parameters or mathematical models [8]. Similarly anti-lock brake wheel-speed sensors are very suitable to determine the vehicle's yaw rate and lateral acceleration in particular areas of operation. Thus using these sensors only along with Kalman approach, two other sensors can be eliminated and the value for the yaw rate and lateral slip velocity can be determined using a mathematical model developed by Venhovens [8]. The mathematical model developed by Venhovens is as shown below in Figure 10.

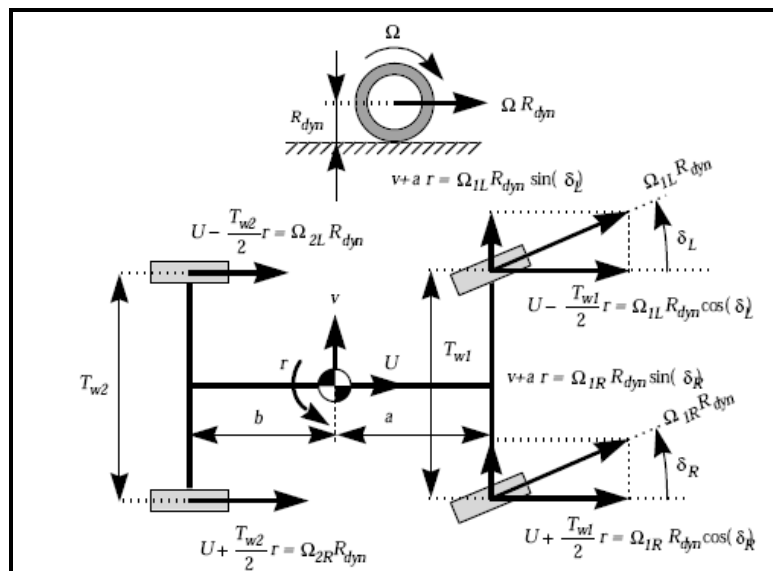


Fig. 10 Mathematical model depicting the relation between vehicle speed, yaw rate and the slip angle [8]

From this mathematical model we can estimate the lateral slip velocity and yaw rate by the following relations defined in Equations (6) - (7):

$$U + \frac{t_w}{2} \cdot r = \Omega_{1R} \cdot R_{dyn} \cdot \cos(\delta_R) \quad (6)$$

$$v + a \cdot r = \Omega_{1R} \cdot R_{dyn} \cdot \sin(\delta_R) \quad (7)$$

where t_w is the track width of the vehicle, r is the yaw rate, R_{dyn} is the dynamic tire radius, v is the lateral slip velocity, a is the distance of the C.G to the front axle and Ω_{1R} is the angular velocity of the front right wheel.

In the absence of wheel speed sensors for the determination of the wheel velocities, the following approach was adopted. During a cornering maneuver vehicle wheels spin with an angular velocity, say for the right wheel, the wheel angular velocity is given by the relation,

$$\Omega_{1R} = \frac{v}{R_{dyn}} \quad (8)$$

For most rollover testing methods, the entry speed for the maneuver is chosen to be 50 mph. Hence from (8) the angular velocities of the wheels can be determined. It is assumed here that the right and left wheel have approximately same angular velocities.

3.3.3 Steering Profile

On the guidelines issued by the US Congress, NHTSA had to incorporate a standard rollover test procedure in its rollover risk assessment of vehicles. In conversant with all major automobile manufacturers NHTSA decided to evaluate test maneuvers based on

their repeatability, discriminatory capability and practicality [19]. A summary of all principal test maneuvers are shown in Table 3.

Table 3 Summary of rollover resistance maneuver scores [19]

Assessment Criterion	NHTSA J-Turn	Fishhook 1a	Fishhook 1b	Nissan Fishhook	Ford Path-Corrected Limit Lane Change	ISO 3888 Part 2 Double Lane Change	Consumers Union Short Course Double Lane Change	Open-Loop Pseudo-Double Lane Change
Objectivity and Repeatability	Excellent	Excellent	Excellent	Good	Bad	Bad	Bad	Satisfactory
Performability	Excellent	Good	Excellent	Satisfactory	Satisfactory	Good	Satisfactory	Satisfactory
Discriminatory Capability	Excellent*	Excellent	Excellent	Excellent	Good	Very Bad	Very Bad	Very Bad
Appearance of Reality	Good	Excellent	Excellent	Good	Excellent	Excellent	Excellent	Excellent

*When limited to vehicles with low rollover resistance and/or disadvantageous load condition.

Source: NHTSA

The force profile chosen for this rollover assessment was the NHTSA Fishhook 1A maneuver. The fishhook maneuver as specified by NHTSA is outlined as below in Figure 11.

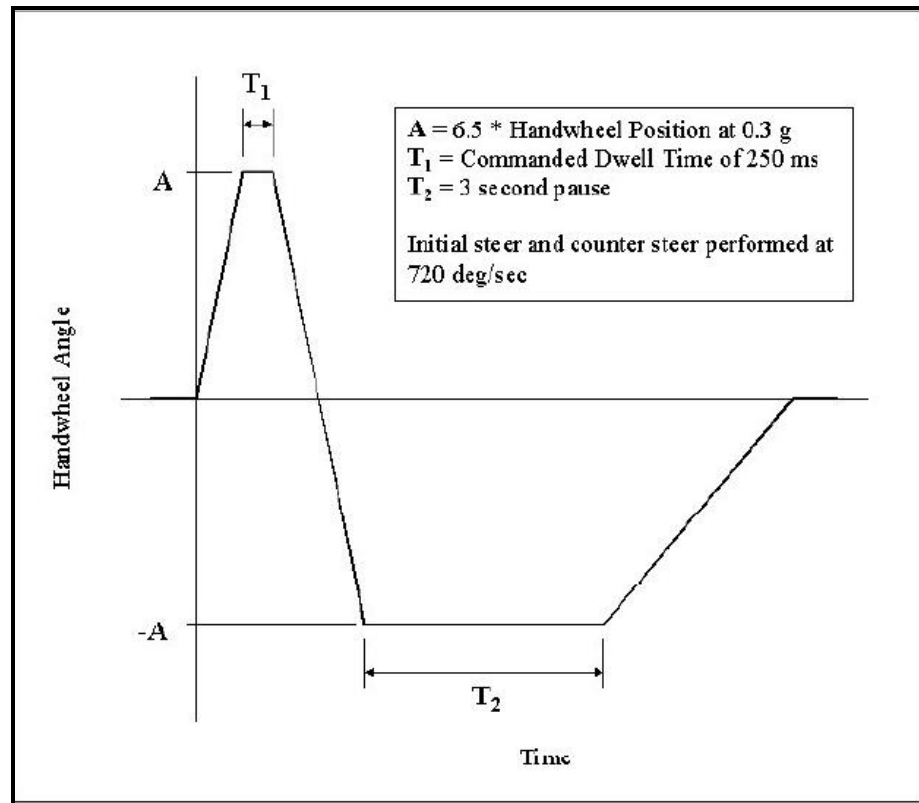


Fig. 11 NHTSA fishhook 1A maneuver description [19]

This maneuver begins with driving the vehicle slightly faster than the desired entrance speed, in this case, 50 mph. The driver then releases the throttle and then turns the steering wheel for the angles mentioned in Figure 11. The hand wheel turning rate both for the counter steer and the initial steer angle is 720 degrees per second. The fishhook maneuver considered for this study included first a right turn amounting to -287 degrees. Then a dwell of 0.25s is maintained in that position and the steering angle is begun to rotate in the opposite direction until it reaches +287 degrees. Then again there is a dwell of 3s at this position after which counter steering is done to return to the normal position. The convention here is that counter clockwise rotation of the front tire angle when viewed from top is considered as positive while the clockwise rotation of the front tire when viewed from top is considered as negative. Hence for a right turn the front tires

would sweep a clockwise angle making the angle negative in magnitude. The fishhook lane change maneuver in which the variation of hand wheel steering angles with respect to time is outlined as in Table 4:

Table 4 Variation of hand wheel steering angle with respect to time

Time (s)	Duration (s)	Steering Angle (degrees)	Description
0-0.3986	0.3986	0→-287	<i>Vehicle making a right turn</i>
0.3986-0.6486	0.25	-287	<i>Maintaining Steady right turn</i>
0.6486-1.4458	0.7972	-287→+287	<i>Making a full left turn from the rightmost position of steering wheel</i>
1.4458-4.4458	3.00	+287	<i>Maintaining left turn</i>
4.4458-6.4458	2.00	+287→0	<i>Counter-steering to neutral position</i>

The hand wheel angle position at 0.3g was taken for a standard automobile as 287 degrees and the following steering profile was simulated in Matlab as shown in Figure 12 and a schematic representation of the maneuver is shown in Figure 13.

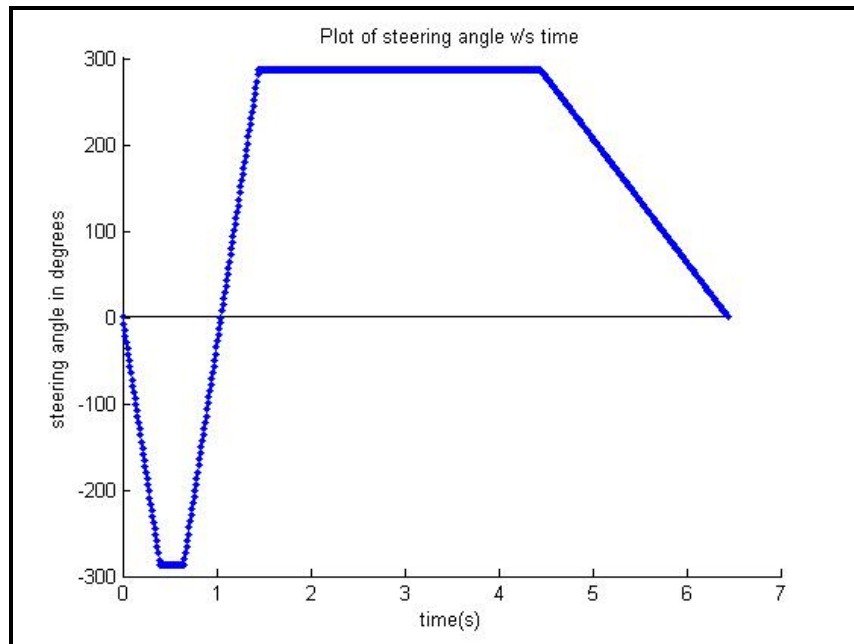


Fig. 12 Fishhook 1a maneuver in Matlab

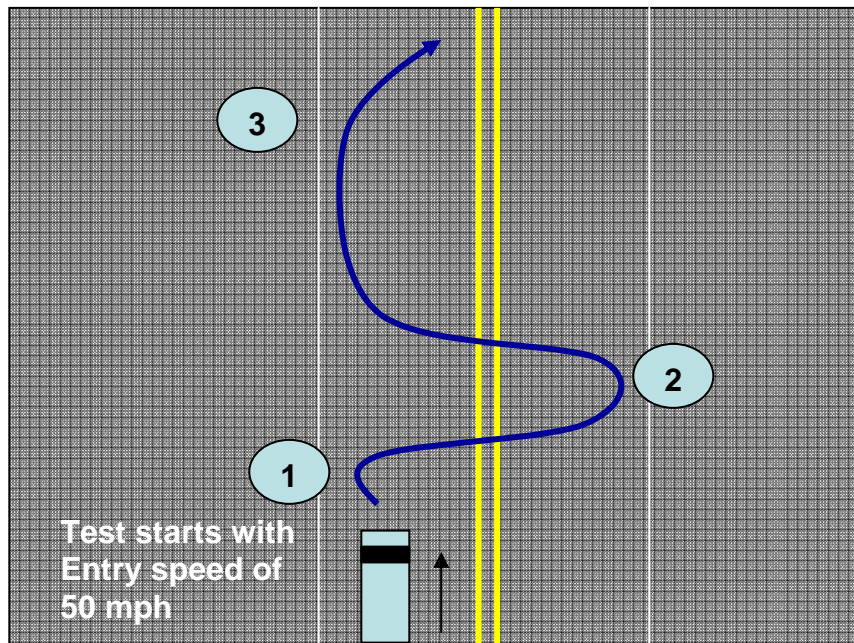


Fig. 13 Graphical representation of fishhook maneuver

In accordance with the steering profile, the yaw rate equations would thus change for the front inner and outer tire as shown below in Figure 14 and Table 5.

The fishhook maneuver considered makes a right turn initially, remains steady and then makes a left turn, remains steady and then counter-steers back to its original neutral position. The yaw rate equations thus would be as follows:

Yaw Rate for a front inner tire making a left turn,

$$r_{11} = \frac{U - (\Omega_{1L} \cdot R_{dyn} \cdot \cos(\delta_L))}{(t_w)/2} \quad (9)$$

Yaw Rate for a front outer tire making a left turn,

$$r_{12} = \frac{(\Omega_{1R} \cdot R_{dyn} \cdot \cos(\delta_R)) - U}{(t_w)/2} \quad (10)$$

Yaw Rate for a front inner tire making a right turn,

$$r_{21} = \frac{(\Omega_{1L} \cdot R_{dyn} \cdot \cos(\delta_R)) - U}{(t_w)/2} \quad (11)$$

Yaw Rate for a front outer tire making a right turn,

$$r_{22} = \frac{U - (\Omega_{1R} \cdot R_{dyn} \cdot \cos(\delta_L))}{(t_w)/2} \quad (12)$$

We consider the Fishhook steering maneuver and divide the profile into a number of forces as shown below in Figure 14. These forces are actually evaluated within the Matlab Code for the corresponding time period and steering angle. However an attempt to give an insight as to how the yaw rates and lateral forces would vary is made in Figure 14 and Table 5. If we discretize each maneuver of the Fishhook into individual forces

then the matrix in Table 5 below shows as to the necessary equations that need to be used as the steering profile changes.

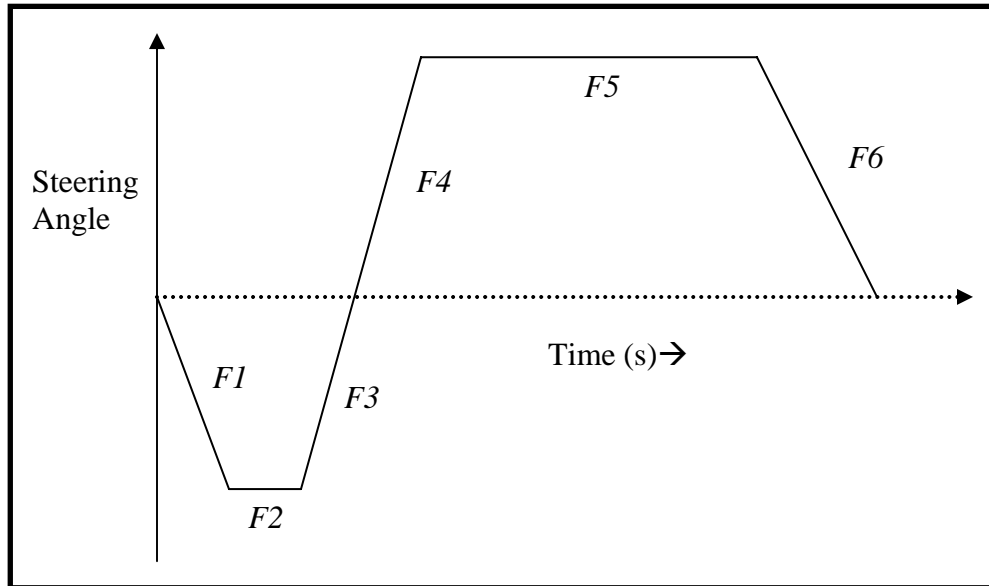


Fig. 14 Lateral force variation for different sections of the steering profile

Table 5 Variation of yaw rates for the front tires with steering profile

	<i>Right Tire</i>	<i>Left Tire</i>
<i>F1</i>	r_{21}	r_{22}
<i>F2</i>	r_{21}	r_{22}
<i>F3</i>	r_{11}	r_{12}
<i>F4</i>	r_{12}	r_{11}
<i>F5</i>	r_{12}	r_{11}
<i>F6</i>	r_{22}	r_{21}

3.3.4 Determination of Cornering Stiffness

The graph of the lateral tire force plotted versus the slip angle is linear for very small slip angles as shown in Figure 15. Beyond a threshold the relationship between the two becomes non-linear. It is in this linear region in our study that it is assumed that the tires are functioning.

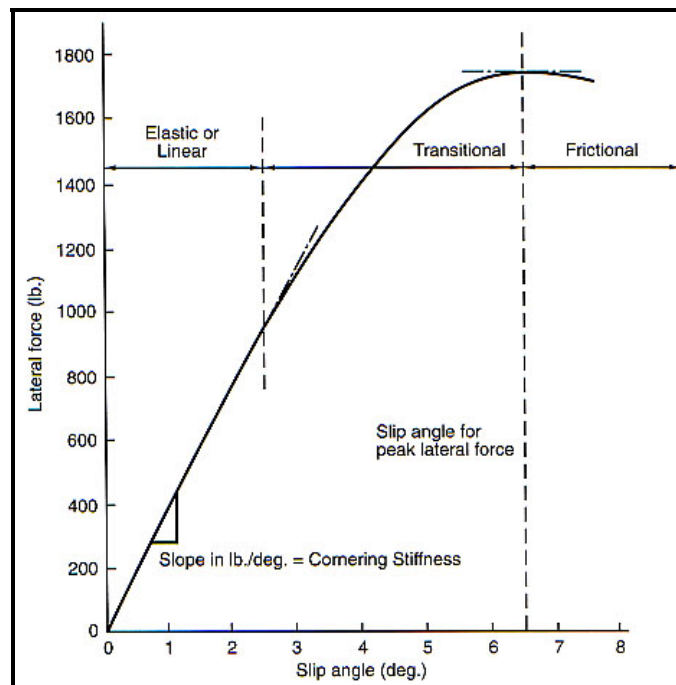


Fig. 15 Lateral force vs. slip angle for a racing tire [20]

The slip angles obtained for this study are very low and the tangents of the angles are in the order of 10^{-1} . From Sienel [21], the dependency of cornering stiffness on the slip angle for a longitudinal speed of 50 km h^{-1} is plotted as shown in Figure 16. From Figure 16, the approximate value of the cornering stiffness for this range of slip angles is estimated to be $7 \times 10^4 \text{ N/rad}$.

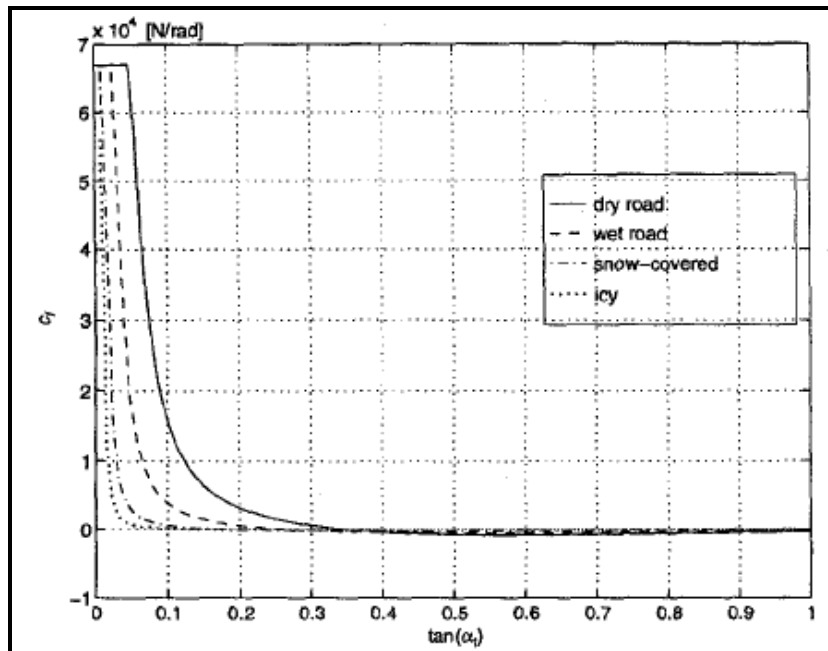


Fig. 16 Dependency of cornering stiffness on slip angle for entry speed of 50 kmph [21]

With the values of cornering stiffness, yaw rate and lateral velocity keyed into the Matlab code which is as shown in Appendix I, the output is the lateral tire forces for both the front left and right tires as it executes a Fishhook 1a maneuver. (4-8) are coded into this Matlab Code for the steering profile shown in Figure 12 and the output profile of the lateral tire forces for both the front tires are obtained as shown in Figure 17 below: The force values are stored into a 'mat' file for later use with the Simulink model that is explained in the subsequent section.

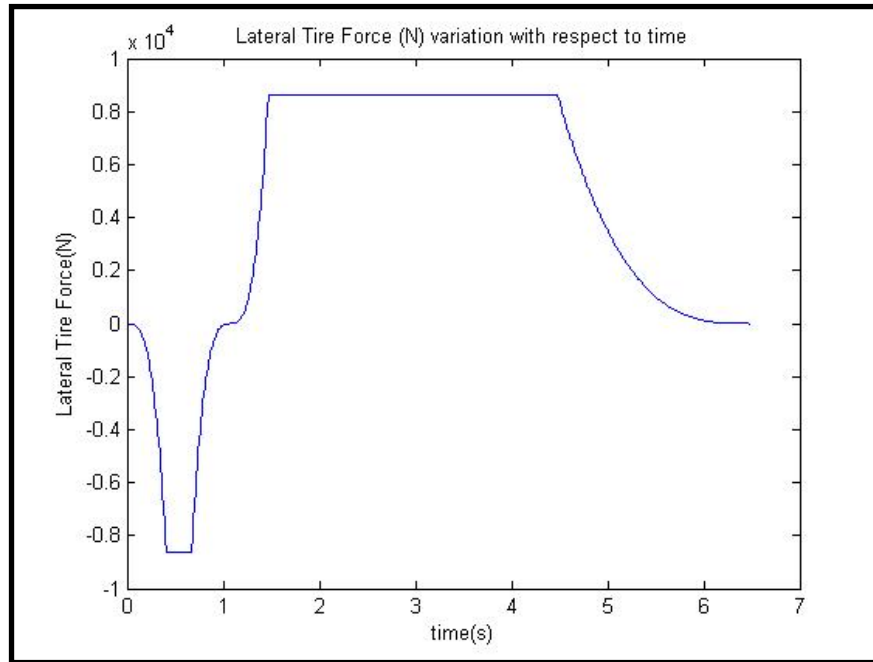


Fig. 17 Lateral front tire forces for the given steering profile

3.3.5 Predictive Modeling

Hyun et al. [22] used a 12 DOF vehicle model to develop a predictive system for rollover in tractor semi-trailers. This predictive model consisting of roll plane models of vehicle sprung and an unsprung mass is used in association with online vehicle parameter identification. The objective of this predictive modeling is to determine Least Time to Rollover (LTR) values for the tractor-semitrailer and compare the same with actual values. By developing such a model it is very easy to predict the rollover behavior.

This predictive model outlined in Hyun [22] was used in this study to plot a regression line between the roll angle and lateral acceleration both obtained through simulations. The regression plot would give two constants, α and β where

$$\alpha = \frac{M \cdot h_2}{(K_s - M \cdot g \cdot h_2)} \quad \text{and} \quad \beta = \frac{M \cdot g \cdot y_0}{(K_s - M \cdot g \cdot h_2)}$$

Solving for these constants we get accurate values for the roll center height, h_2 and the lateral shift in the C.G of the body, y_0 as the vehicle rolls over. The regression plot is as shown in the Figure 18 below:

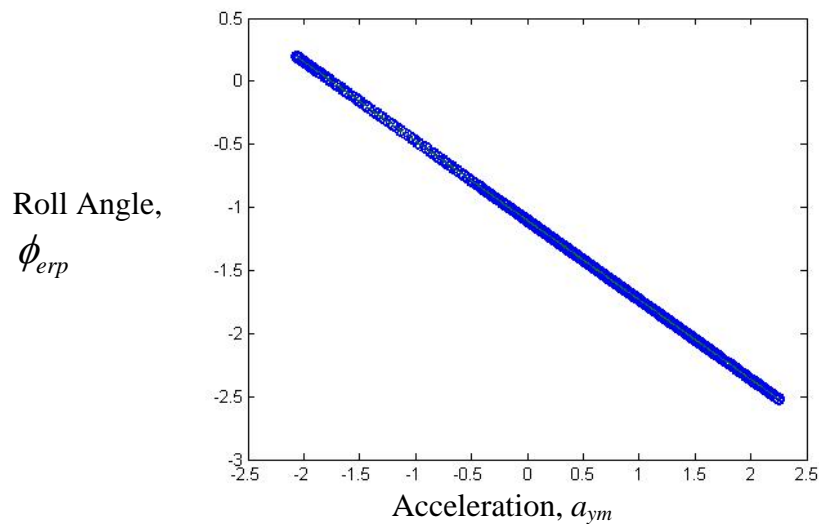


Fig. 18 Regression plot of roll angle and lateral acceleration

3.3.6 Simulink Model

The resourcefulness of Dymola lies in its software migration capability. The model that was developed in Dymola could be plugged into a Simulink model which would accept the lateral tire forces generated as a result of the Matlab Code as input. The lateral force input would be compiled by the Dymola model and the lateral acceleration sensor would

output the values to Matlab workspace through the *outPort1* present in the Dymola model.

The Simulink Model is as shown in Figure 17. It primarily consists of the Dymola block which has four input parameters to it i.e. the front left and right lateral tire forces and the two vertical forces. The front left and right lateral tire forces are generated as an output of the Matlab Code. The front vertical right and left tire forces are calculated from the following two relations shown in Equations 13 and 14:

$$F_r = \frac{W}{2} + \frac{M \cdot a_{ym} \cdot h}{t_w} \quad (13)$$

And

$$F_l = \frac{W}{2} - \frac{M \cdot a_{ym} \cdot h}{t_w} \quad (14)$$

During cornering, the vertical forces on the outer tires increase at the expense of those on the inner ones. The transfer of vertical force is called “lateral load transfer”, As can be seen from Equations (13)- (14), the lateral load transfer is a function of the lateral force acting on the vehicle, the track width and also the height of the center of gravity of the vehicle.

In the Simulink model shown in Figure 19, the lateral acceleration values are fed back into the loop to increase the accuracy of the vertical tire forces. The vertical tire forces are then used as input to the Dymola block.

The Dymola block now has four inputs. The two suspension relative position sensors present in the Dymola model are output through *outPort2* and *outPort3* (Refer Figure 7).

Hence modifying Figure 9, the Dymola block could be shown as a four input- three output system. The two suspension relative position sensor values are subtracted to give the overall deflection of the suspension system and that value is subsequently used to calculate the roll angle induced by the suspension movement. Equation (1) is used to calculate the roll angle caused by the suspension movement. It is to be noted that since Equation (1) has a lateral acceleration component in it, when the vehicle is not cornering and is traveling on a straight road, the roll angle component from suspension movement is sufficiently small. The lateral acceleration values and the relative suspension movement values are output to the workspace of Matlab which is further written into an ASCII text file for further analysis. The essential purpose served by the Simulink model was to obtain lateral acceleration values as a function of steering angle input. The values obtained by this method are now used by a rollover identification system designed in LabVIEW.

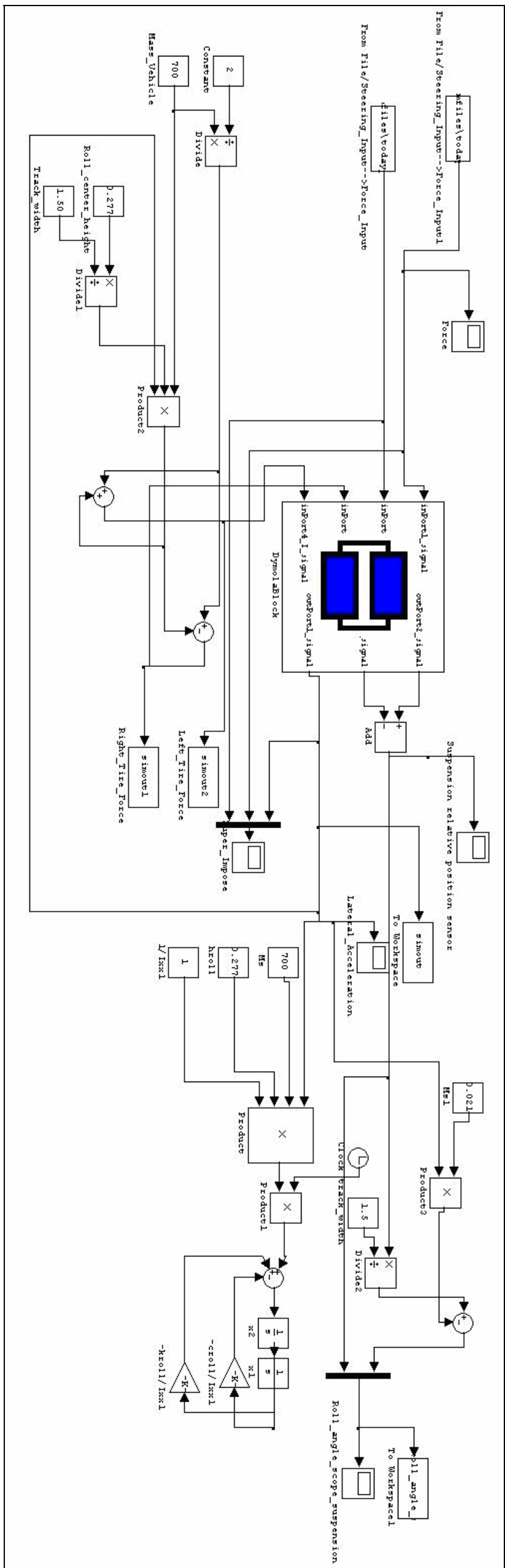


Fig. 19 Simulink model connecting Dymola and the Matlab code to generate lateral acceleration values as the output

CHAPTER IV

ROLLOVER IDENTIFICATION SYSTEM

4.1 Software Integration

Before the rollover identification system is discussed, it is very essential to indicate the software integration that was done for this study.

- i) Firstly, a simple semi-car model was developed in Dymola consisting of sprung and unsprung masses, suspensions systems modeled as spring-damper systems, tires modeled as springs, suspension relative position sensors to measure the deflection of the suspension and a lateral acceleration sensor to measure the lateral acceleration generated due to the lateral tire forces.
- ii) Relation between the steering angle and the lateral force generated at the wheels was established using the Matlab Code.
- iii) The Matlab Code made use of a standard NHTSA maneuver testing procedure to model the various tire forces for the given steering profile.
- iv) The Simulink model developed integrated the above three steps and generated lateral acceleration and suspension deflection as its output parameters.
- v) These parameters were stored into a file and then is subjected to analysis using a LabVIEW enabled Rollover Identification System.

The software integration is schematically represented in Figure 20 below.

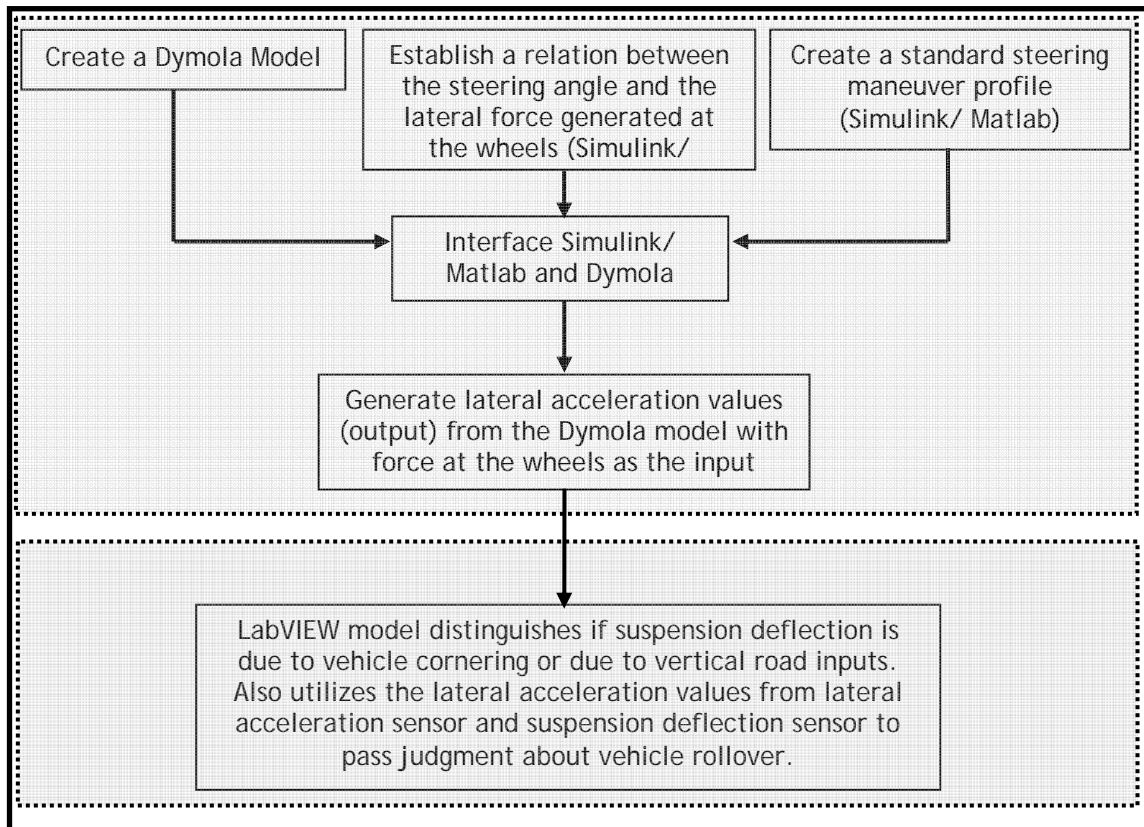


Fig. 20 Data flow within the software integration

4.2 Reasons for Choosing LabVIEW

The values of lateral acceleration and roll angle generated as described in the previous section. The whole purpose of this study was to determine rollover that may be maneuver induced or through road inputs or through both. In the absence of an actual test bench, the values of lateral acceleration and suspension relative movement needed to be simulated for which Dymola/ Matlab Simulation was used. Since such an integration of sensors would have brought ambiguity for different driving conditions, an identification system needs to be established. For this a LabVIEW model was developed over Matlab animation toolbox for the following two reasons:

- 1) In case of an actual implementation, LabVIEW can very easily be interfaced with sensors since it is primarily a data acquisition system software. As for now the LabVIEW software gets its input from a text file of values. In actual implementation, these values could be had from an actual system of sensors. Hence LabVIEW was used.
- 2) Use of ease- LabVIEW has many functions very suitably built into the software which enables the development much easier.

4.3 Rollover Identification System

The front end view of the rollover identification system designed in LabVIEW is as shown in Figure 21. The rollover identification system reads the input files of lateral acceleration and relative suspension movement values generated in the previous step of Simulink model as shown in Figure 22.

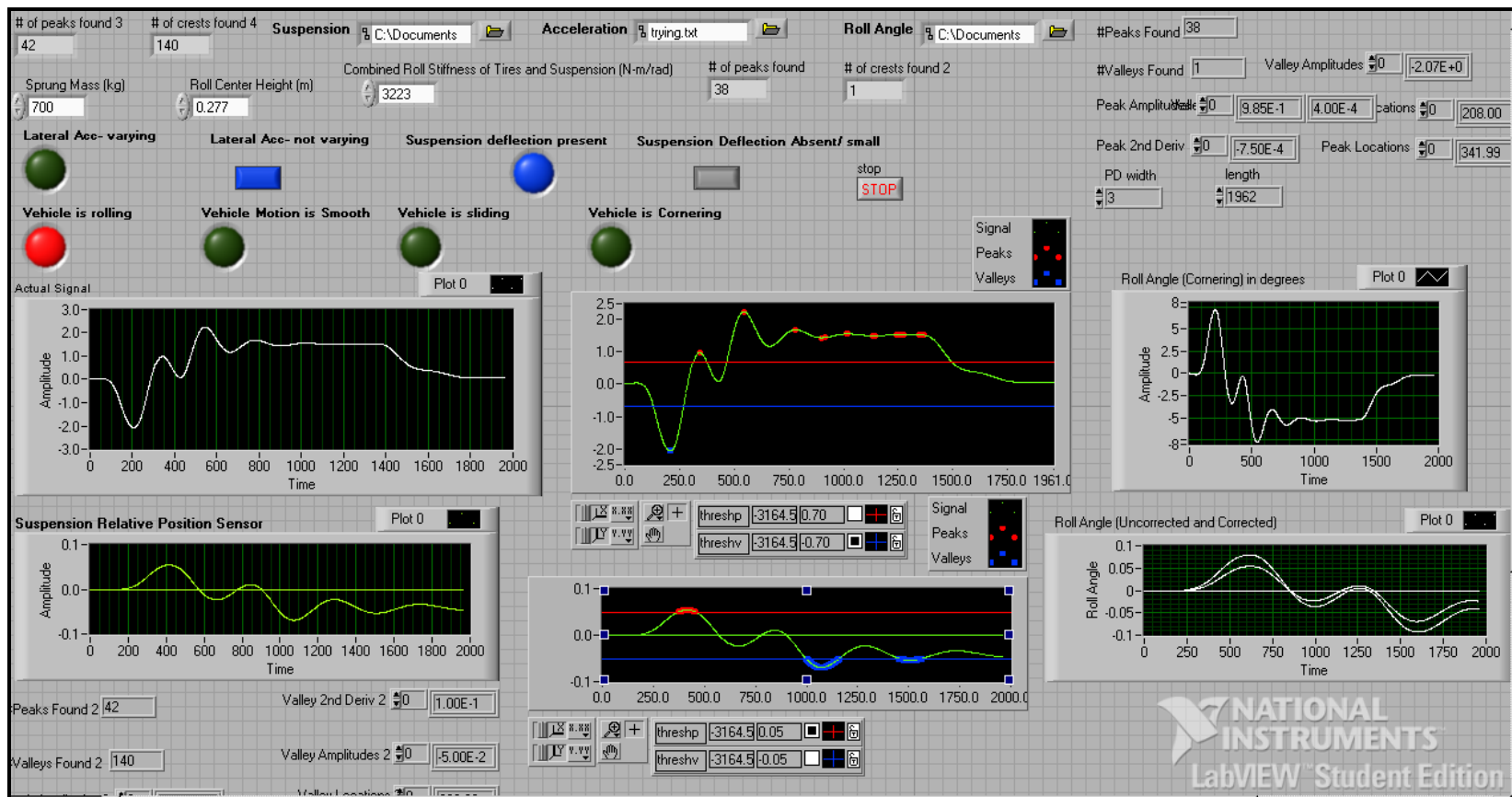


Fig. 21 Front panel of the rollover identification system

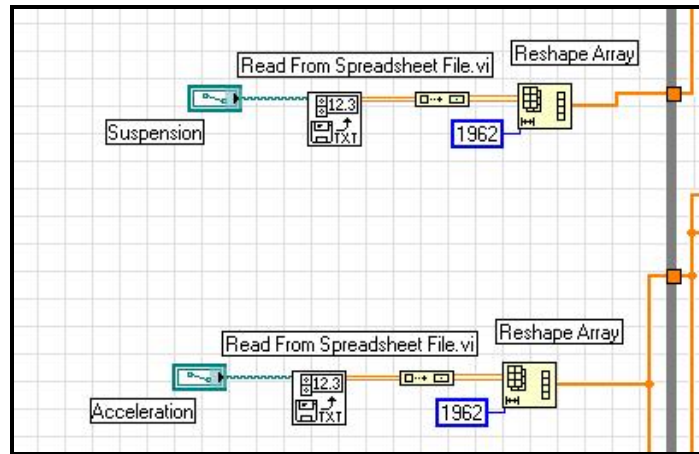


Fig. 22 Rollover identification system reading input files from Simulink

The acceleration values are first plotted in the “Actual Signal” window. These values are then taken inside a “while” loop where the values are passed through a peak detector. The essential function of a peak detector is to detect the number of peaks/ valleys, to indicate the positions at which these peaks are found and also to display the amplitude of these peaks. The number of peaks detected by the peak detector is based on the threshold set by the user. This is achieved by using a property node through which the cursor on the graph could be positioned to indicate the high and low value of the threshold range. Figure 23 shows a peak detector and a property node.

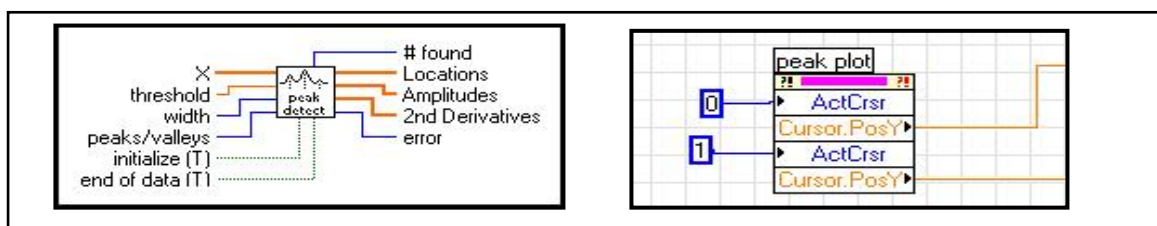


Fig. 23 Peak detector and property node

The number of peaks/ valleys detected by the peak detector depends on the threshold range that is set by the user. For the given acceleration profile, if a small threshold range of 0.3g is set, then the number of peaks/ valleys detected would be naturally high.

Whereas very high threshold values would lead to lesser number of peaks/ valleys detection.

A similar approach is used for the suspension relative position sensor values. The number of peaks/ valleys detected would depend upon the threshold value set for the suspension movement.

With the number of peaks/ valleys detected, it is now desired to estimate if there is any variation in the lateral acceleration and whether the lateral acceleration exceeds a set threshold. This is achieved by passing through another “while” loop in which the number of peaks/ valleys detected is compared against a set value. This set value would be the minimum value beyond which if peaks/ valleys are detected, then we concur that the lateral acceleration is varying.

Now there could be two cases: 1) that the number of peaks/ valleys exceeding the threshold is greater than the set value 2) that the number of peaks/ valleys exceeding the threshold is not greater than the set value. If the peaks/ valleys either or both exceed the set value, then we can surely say that the lateral acceleration is varying. If both the peaks/ valleys do not exceed the set value would indicate that the lateral acceleration is not varying. A similar Boolean logic is created for the suspension relative position sensors where the output has to be that the suspension deflection is either present or absent. This is summarized in Table 6 below:

Table 6 Summary table for determining presence of suspension deflection or variation of lateral acceleration

Peaks > exceed set value	Valleys > exceed set value	Comments
✓	✘	<i>Lateral Acceleration is varying or suspension deflection is present</i>
✘	✓	<i>Lateral Acceleration is varying or suspension deflection is present</i>
✓	✓	<i>Lateral Acceleration is varying or suspension deflection is present</i>
✘	✘	<i>Lateral Acceleration is not varying or there is no suspension deflection</i>

From the above logic there could be four different types of cases. These cases are summarized below. These cases would be dealt in detail in the next section of results and discussion. The indicators associated with these cases would glow on the front end of the LabVIEW program give a fair indication as to what is causing the change in the dynamics of the vehicle.

Case 1:

Suspension Deflection present; lateral acceleration is not high/ does not vary rapidly.

Case 2:

Suspension deflection is present; lateral acceleration is high and varying rapidly.

Case 3:

Suspension deflection is absent/ small; lateral acceleration is not high/ does not vary rapidly.

Case 4:

Suspension deflection absent/ small; lateral acceleration is high and varying rapidly.

Based on the indicator glows, the type of vehicle motion that is being induced i.e. is the vehicle cornering, rolling, sliding or is smooth could be determined. Based on this the corresponding equations for the roll angles are used to determine the roll angle and roll rate.

CHAPTER V

RESULTS AND DISCUSSIONS

Rollover in vehicles is increasingly becoming a critical issue. With more and more fatalities occurring due to rollover, it is very essential that we identify all parameters that cause rollover and try to prevent the same by active control.

De-stabilization of the C.G of the vehicle is either maneuver induced or due to road based inputs. An ideal rollover system should be capable of identifying both these inputs and should also be able to differentiate between the same. In this study, an attempt is made to combine the outputs from two sensors and couple them in such a way that rollover identification can be done.

5.1 Dymola and Simulink Models

In order to generate lateral acceleration and suspension relative position sensor values, a semi-car model was developed in Dymola. The inputs to this Dymola model are the lateral tire forces which are calculated based on steering angle as the input. The variation of yaw rate, steering angle, lateral tire forces with respect to time are plotted and are as shown in Figures (24-26).

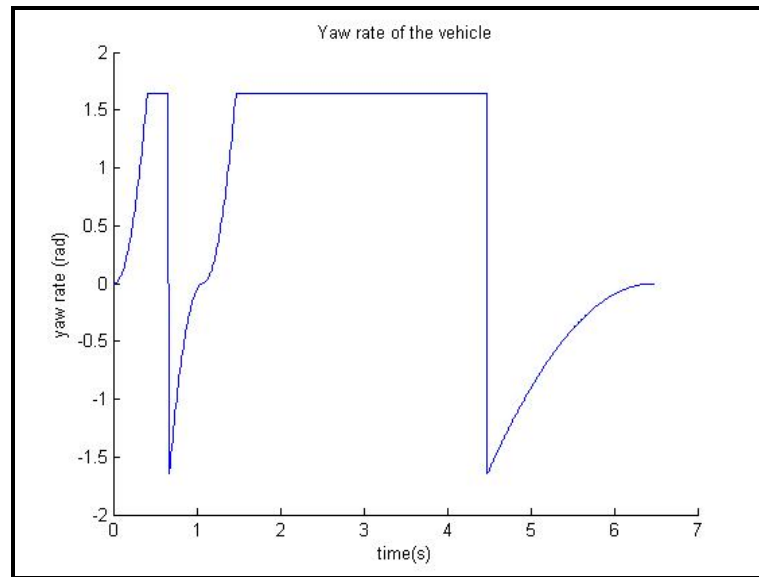


Fig. 24 Yaw rate of the vehicle

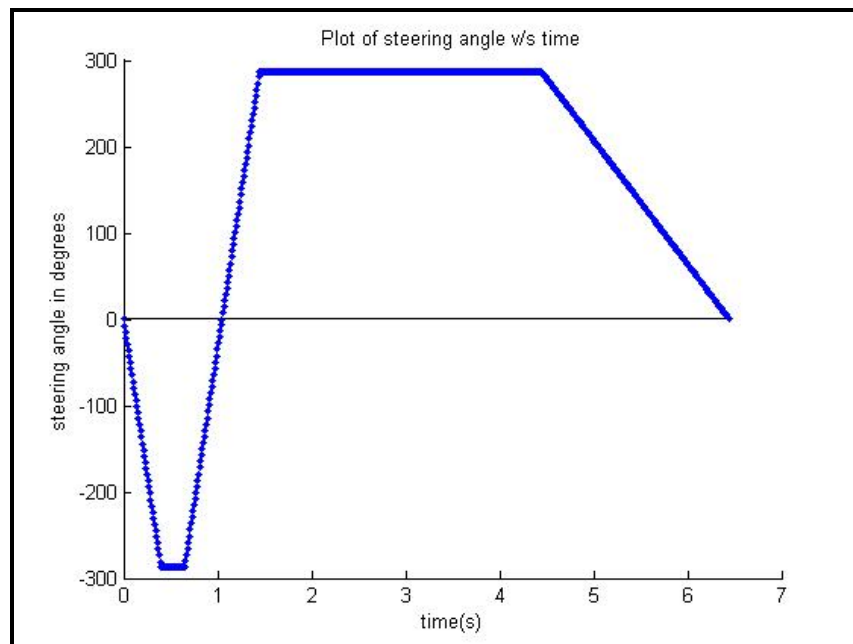


Fig. 25 Steering angle vs. time

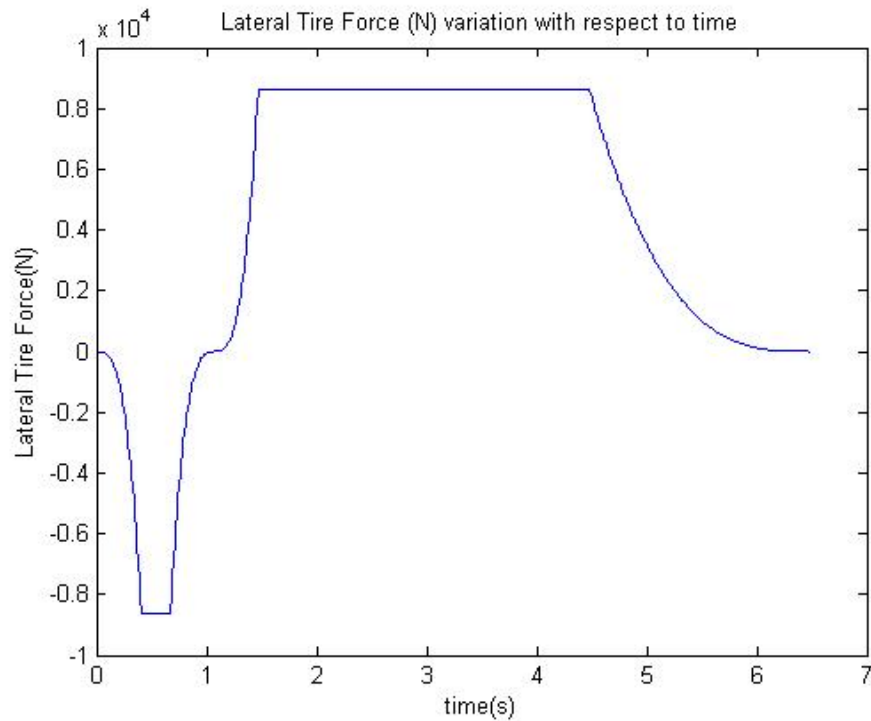


Fig. 26 Variation of lateral tire force (N) vs. time

The maneuvers are performed for a dry road with a constant speed of 50 km h^{-1} . The variation of lateral tire force with respect to slip angle is assumed to be in the linear region.

When the values of the lateral tire forces generated from the Matlab Code are input into the Simulink Model, we get the variation of the lateral acceleration during the entire maneuver and also the relative movement of the suspension system as measured by the suspension relative position sensor. The suspension movement is relatively small as the vehicle is cornering at quite a high rate and the suspension movement that is obtained is primarily due to cornering. Figures (27-28) demonstrate the variation of lateral acceleration and relative suspension movement with respect to time.

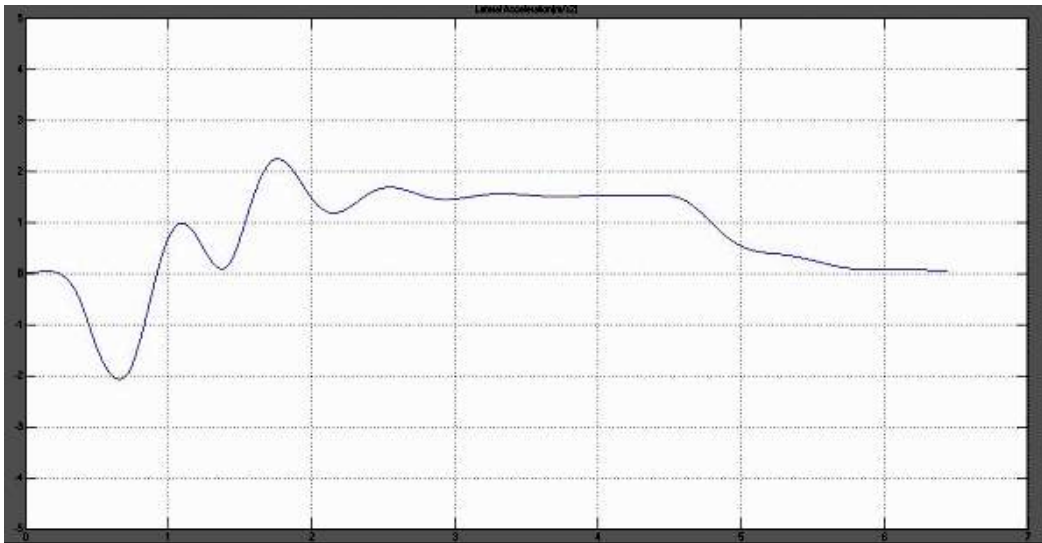


Fig. 27 Variation of lateral acceleration vs. time

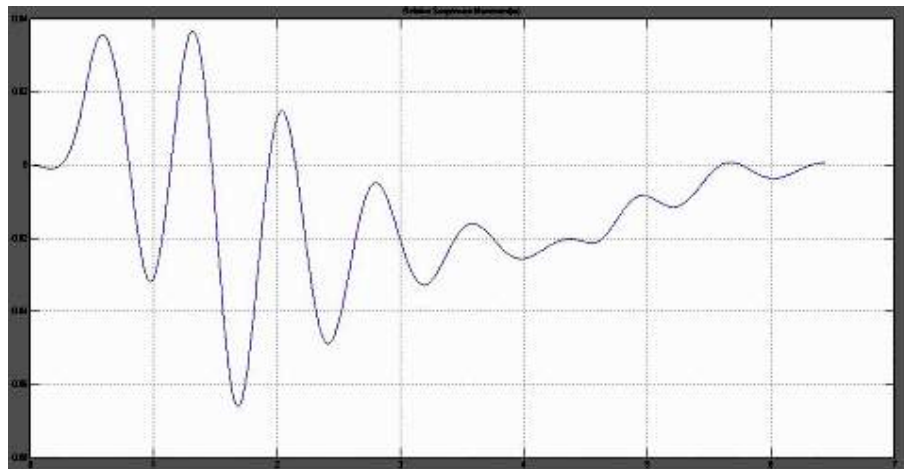


Fig. 28 Relative suspension movement vs. time

It can be clearly observed from Figures (27-28) that when the lateral acceleration increases, the relative suspension movement increases resulting in larger displacement resulting in a local maxima. This is primarily due to lateral load transfer that occurs during cornering.

Using Hyun [22] predictive modeling technique, the regression line is drawn between roll angle and lateral acceleration. The regression constants helps to determine the accurate roll center height and the shift in the lateral distance of the C.G. An ANOVA analysis was done on the data obtained to verify if it contained any outliers. The roll angle was re-plotted with the accurate values of roll center height. The plots for regression analysis, ANOVA analysis and roll angle calculations are plotted in Figures (29-31).

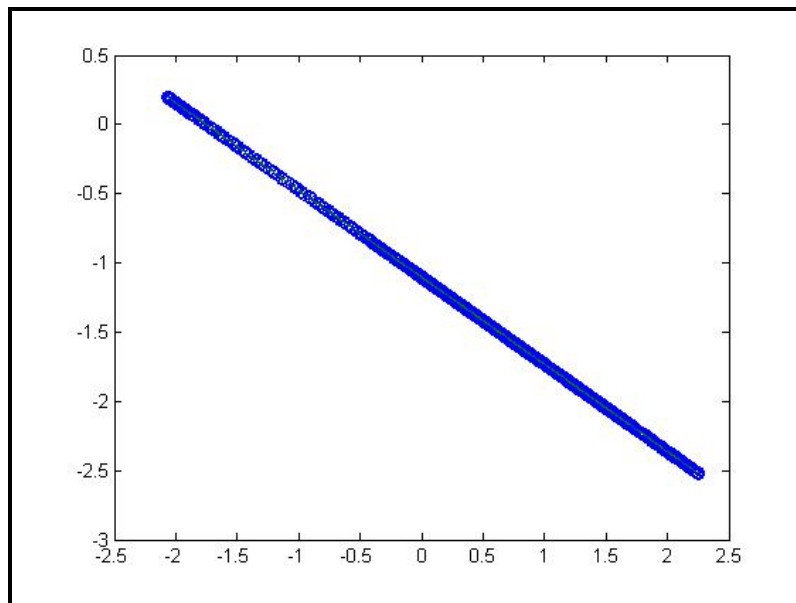


Fig. 29 Linear regression line plotted for roll angle and lateral acceleration.

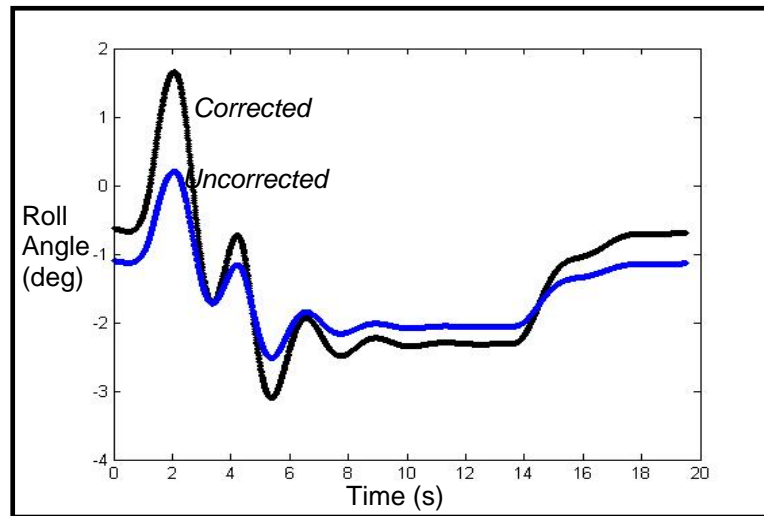


Fig. 30 Plot of original roll angle (without the uncorrected roll center height and lateral shift in C.G) and corrected roll angle

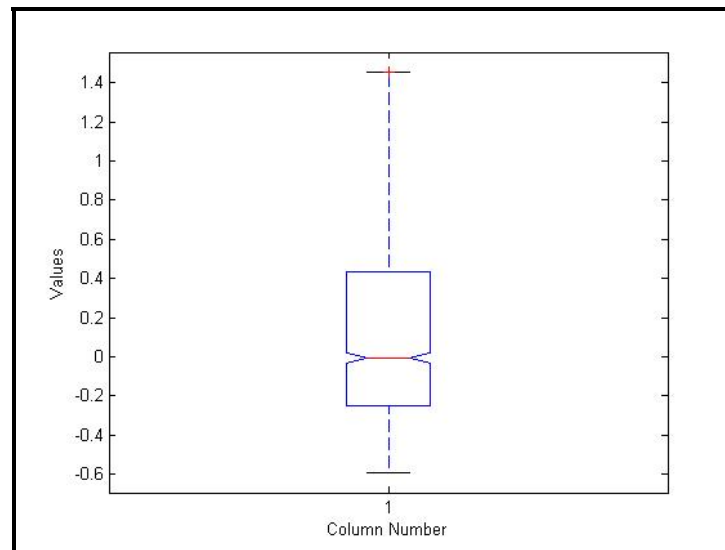


Fig. 31 ANOVA analysis on roll angle data

Using the expressions defined by Hyun, the Least-time to rollover was determined for the Dymola model. The LTR should fall between -1 and +1. The LTR defines the two wheel lift off condition (TWLO). For the Dymola model as seen in Figure 32, the LTR

falls between -0.5 and +0.5 indicating that for the accelerations developed in this maneuver, TWLO condition is not seen.

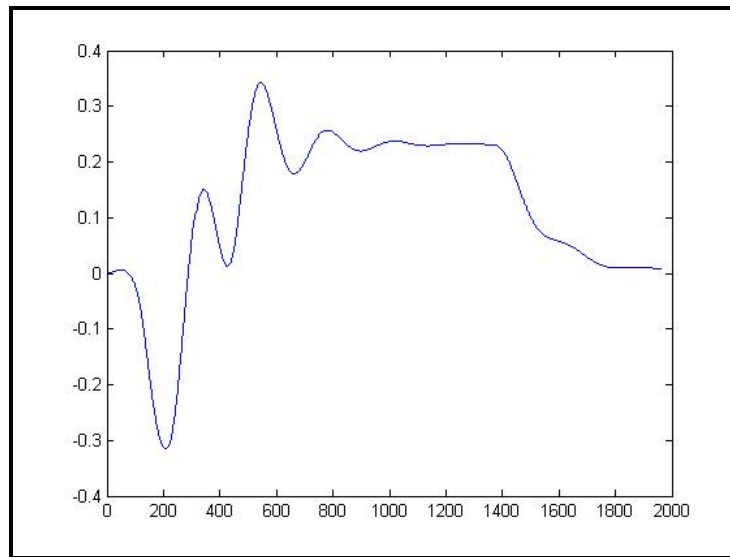


Fig. 32 LTR for the Dymola model

5.2 Rollover Identification System

The rollover identification system was developed in LabVIEW and its principal objective was to differentiate different types of inputs that would cause a change in the parameters of the vehicle and pass judgment as to whether the vehicle is prone to rollover or not.

In the earlier section four different cases were mentioned and identification of each of these four cases would bring about a complete rollover identification module. Outlined

below are the four different cases and also their associated indicators are demonstrated. It can clearly be seen that the system is able to identify between two different types of inputs which have completely different effects on the vehicle.

Case 1

Suspension Deflection present; lateral acceleration is not high/ does not vary rapidly.

This may arise due to unevenness in roads like potholes and bumps. Bumps and holes may cause deflection but there would be no change in lateral acceleration. Hence the lateral acceleration indicator does not vary rapidly. Roll angle is calculated using Equation (2) albeit with a negative sign. This is because this equation is used only when the suspension deflection is caused by vertical road inputs. The indicator on the front panel would only light up when the suspension deflection is due to road inputs. It is only after this indicator lights up that the roll angle is calculated using Equation (2) with a negative sign. Any ambiguity that this roll is created by virtue of cornering is eliminated. The array of indicators would glow as shown in Figure 33 below.



Fig. 33 Front panel indicators for case 1

Case 2:

Suspension deflection is present; lateral acceleration is high and varying rapidly.

If there is a suspension deflection and a variation/ and high values of lateral acceleration, then it can be inferred that cornering is the cause for these values and Equation (1) and (2) could be suitably used to estimate the roll angle. The indicator in this case would only light up when there is suspension deflection and variation in lateral acceleration. The array of indicators would glow as shown in Figure 34 below.



Fig. 34 Front panel indicators for case 2

Case 3:

Suspension deflection is absent/ small; lateral acceleration is not high/ does not vary rapidly.

If there is a small/ negligible suspension deflection is indicative that the vehicle is going on a smooth road and added if there is no variation/ high values of 'g' then it can be inferred that the vehicle is neither cornering nor going on a rough road. The indicator combination is as shown below in Figure 35.



Fig. 35 Front panel indicators for case 3

Case 4:

Suspension deflection absent/ small; lateral acceleration is high and varying rapidly

If there is very little suspension deflection and yet we have very high values of lateral acceleration, then it may be the case in which the vehicle is sliding away as a rigid body on a very low friction surface without bringing any change in the deflection of the spring. The indicator combination is as shown below in Figure 36:



Fig. 36 Front panel indicators for case 4

The Dymola model developed earlier is able to simulate a steady state cornering car and obtain good values for the lateral acceleration and the suspension relative position sensors. It can also be concluded that the objective of identifying both maneuver induced

and road input induced disturbances are recognized by the LabVIEW based Rollovers Identification System.

CHAPTER VI

SUMMARY AND FUTURE WORK

An attempt has been made in this study to model the semi-car dynamics using a new vehicle dynamics simulation software called Dymola. The Dymola was innovatively used not only to model the vehicle but also an interface was created between Matlab/Simulink and Dymola. The Dymola software is still largely unexplored. The semi-car model that was created utilized the translational mechanics toolbox in the software. Actual automobile prototypes could be built with in-built vehicle dynamics toolboxes where actual vehicle components exist with their appropriate material and structural properties.

A complete car model developed within Dymola could possibly ease the understanding of rollover and help it to predict and prevent rollover in vehicles.

Also the suspension and tires were assumed to be linear in operation. Design of vehicles with non-linear suspensions should be modeled. Most driving situations especially rollover are basically non-linear state. An attempt to model the non-linear behavior during rollover could be made.

REFERENCES

1. Automobile Business Report 2004, Honda Corporation, Torrance, CA.
2. NHTSA's National Center for Statistics and Analysis "NHTSA 2004 Projections on Motor Vehicle Traffic Crash Fatalities and Injuries", DOT HS 809 862, April 2005
3. NHTSA Vehicle Research and Test Center, Vehicle Dynamic Rollover Propensity, <http://www-nrd.nhtsa.dot.gov/vrtc/ca/rollover.htm>, accessed on 18 July, 2005.
4. Gillespie, T., March 1992, *Fundamentals of Vehicle Dynamics*, SAE International, Warrendale, PA.
5. Greene, M., and Trent, V., 2002, "A Predictive Rollover Sensor," SAE Paper No. ADSC 2002-01-1605.
6. Hac, A., Brown, T., and Martens, J, 2004, "Detection of Vehicle Rollover," SAE Paper No. 2004-01-1757.
7. Hegazy, S., Rahnejat, H., and Hussain, K., 2000, "Multi-Body Dynamics in Full-Vehicle Handling Analysis under Transient Maneuver," *Vehicle System Dynamics*, **34**, pp. 1-24.
8. Venhovens, P., and Naab, K., 1999, "Vehicle Dynamics Estimation Using Kalman Filters," *Vehicle System Dynamics*, **32**, pp. 171-184.
9. Huang, C., and Lin, J., March 2004, "Nonlinear Active Suspension Control Design Applied to a Half-Car Model," *Proceedings of the 2004 IEEE International Conference on Networking, Sensing & Control*, Taipei, Taiwan.
10. Schubert, P., Nichols, D., Wallner, E., Kong, Henry and Schiffmann, J., 2004, "Electronics and Algorithms for Rollover Sensing," SAE Paper No. 2004-01-0343.
11. Hac, A., 2005, "Influence of Chassis Characteristics on Sustained Roll, Heave and Yaw Oscillations in Dynamic Rollover Testing," SAE Paper No. 2005-01-0398.

12. Hac, A., and Bodie, M., 2002, "Improvements in vehicle handling through integrated control of chassis systems," *Int. J. of Vehicle Autonomous Systems*, **1**(1), pp. 83-110.
13. Odenthal, D., Bunte, T., Ackermann, J., 1999, "Nonlinear Steering and Braking Control for Vehicle Rollover Avoidance," *European Control Conference*, Karlsruhe, Germany.
14. Ackermann, J and Odenthal, D., July 1998, "Robust steering control for active rollover avoidance of vehicles with elevated center of gravity," *Proceedings of International Conference on Advances in Vehicle Control and Safety*, Amiens, France, 1998.
15. Johansson, B and Gafvert, M., December 2004, "Untripped SUV Rollover Detection and Prevention," *43rd IEEE Conference on Decision and Control*, Paradise Island, Bahamas.
16. Lewis, A.S., and Gindy, M., 2003, "Sliding Mode Control for Rollover Prevention of Heavy Vehicles Based on Lateral Acceleration," *Heavy Vehicle Systems*, A Special Issue of the *Int. J. of Vehicle Design*, **10**(1)(2), pp. 9-34.
17. Ackermann, J and Odenthal, D., 1999, "Damping of Vehicle Roll Dynamics by Gain Scheduled Active Steering", *Proceedings Of European Control Conference*, Karlsruhe, Germany.
18. Kiencke, U., and Nielsen, L., 2000, *Automotive Control Systems - for Engine, Driveline and Vehicle*, Berlin; New York: Springer; Warrendale, PA: SAE International, c2000.
19. Forkenbrock, G., Garrott, W., Heitz, M., and O'Harra, B., 2002, "A Comprehensive Experimental Examination of Test Manuevers That May Induce On-Road, Untripped, Light Vehicle Rollover – Phase IV of NHTSA's Light Vehicle Rollover Research Program," DOT-HS-809-513, U.S. Department of Transportation, National Highway Transportation Safety Administration, Washington D.C.

20. Milliken, W., and Milliken, D., 1995, *Race Car Vehicle Dynamics*, SAE International, Warrendale, PA.
21. Siemel, W., December 1997, "Estimation of the Tire Cornering Stiffness and Its Application to Active Car Steering," *Proceedings of the 36th Conference on Decision and Control*, San Diego, CA.
22. Hyun,D., and Langari, R., 2003, "Modeling to Predict Rollover Threat of Tractor-Semitrailers," *Vehicle System Dynamics*, **39** (6), pp. 401-414.

APPENDIX-I

NOMENCLATURE

C_{Fa1}	Steady state cornering stiffness
F_r, F_l	Right and Left Vertical Tire Forces
F_{y1}	lateral tire force at the front tire
I_{xx1}	Moment of Inertia
K_s	Roll Stiffness of the entire vehicle suspension
M	Mass of the vehicle
R_{dyn}	dynamic tire radius
U	forward vehicle speed
W	Weight of the vehicle
a	distance of the C.G to the front axle
a_{ym}	Measured lateral acceleration
c_{roll}	Combined roll damping of suspension and tires
h	Height of the C.G of the vehicle
h_{roll}	height of the center of gravity of the vehicle above the roll axis
h_2	Vehicle C.G above the roll center
i_{st}	steering gear ratio
k_{roll}	Combined roll stiffness of suspension and tires
$k_{tiresroll}$	Roll stiffness resulting due to tire stiffness
r	yaw rate
$r_{11}, r_{12}, r_{21}, r_{22}$	Yaw rates for the front inner tire making a

	left turn, outer tire making a left turn, inner tire making a right turn and outer tire making a right turn.
t_w	Track width of the vehicle
y_o	lateral shift in the C.G of the vehicle from its longitudinal axis
v	lateral slip velocity
$\Delta z_{LF}, \Delta z_{RF}, \Delta z_{LR}, \Delta z_{RR}$	Suspension deflections at left front, right front, left rear and right rear respectively
Ω_{1L}	angular velocity of the front left wheel
Ω_{1R}	angular velocity of the front right wheel
α_1	Front tire slip angle
δ	steering angle
δ_R	steering angle at the front right wheel
ϕ_{erp}	Roll angle measured through suspension deflection

APPENDIX-II

MATLAB CODE FOR CALCULATION OF LATERAL TIRE FORCES USING STEERING PROFILE AS THE INPUT

```

%The first half of the code calculates the tire forces for a left tire as
%it makes a right turn (when it becomes the outer tire) and left turn (when
%it becomes the inner tire)
clc
clear all
syms x
Cf1=7.0*10e4; %Front tire cornering stiffness (N/rad)
R_dyn=0.3; %Dynamic Tire Radius(m)
i_st=15; %Steering system gear ratio
% According to DOT, for a speed of 64.5 mph, the radius of the horizontal
% curve is about 2500 feet. Hence a speed of 71mph, 10% more than the safe
% limit is assumed.
%R=2500; % Units are in feet
%E=0; % Superelevation is assumed to be zero
%V=((-0.03*R)+((0.03*R)^2+4*R*(15*(E/100)+3.6))^0.5)/2; % Units are in mph
V_speed=50;%units are in mph
V_final=50*0.44704; %units converted into m/s
%V_final=1.10*V
%omega_tires=(V_final/(R_dyn) %Speed is converted from mph to m/s and radius is
converted from feet to meters. Units are rad/s.
%Breadth of vehicle=b
m_v=2000;
%R1=R*0.3048; %Units are in meters
a=1.4; %distance c.g to front axle

```

```

b=1.50; %track width of the vehicle
%h_o=0.183 %height of the vehicle C.G above the ground
%g = 9.81 %acceleration due to gravity in m/s2
%R=((V_final*V_final)*2*h_o)/(0.8*g*b); %here it is assumed that the fishhook
maneuver turns to 287 degrees with +sign for a right turn
%omega_sys=V_final/R;
%R_i=R-(b/2); %assuming no vehicle body side slip angle
%V_i=R_i*omega_sys;
%R_o=R+(b/2);
%V_o=R_o*omega_sys;
omega1_l=V_final/R_dyn;
omega1_r=V_final/R_dyn;
U=V_final; %Forward speed of the vehicle in m/s
%Tw1=1.5; %track width of the vehicle
F=[];
F1=[];
F2=[];
F3=[];
F4=[];
F5=[];
F6=[];
X=[];
r1=[];
r2=[];
r3=[];
r4=[];
r5=[];
r6=[];
for i=0:0.01:0.3986

```

```

delta=(720*-i)*(pi/180);
x=delta/i_st;
r=(U-(omega1_r*R_dyn*cos(x)))/(b/2); %determines the yaw rate of the vehicle
(rad/s)
v=(omega1_l*R_dyn*sin(x)-(a*r));% lateral velocity of the vehicle (m/s)
% fzero(@ (a) (2*Cf1*a)+m_v*omega1_l*R_dyn*cos(x)*tan(x-a),2000); %Evaluating
front tire slip angle, a (rad)
%F0=-2*Cf1*fzero(@ (a) (2*Cf1*a)+m_v*omega1_l*R_dyn*cos(x)*tan(x-a),2000);
%Evaluating the front left(inner) tire lateral force (N)
a1=((v+a*r)/U)-x; %slip angle of the front wheel (rad)
F0=-2*Cf1*a1;
F1=[F1; F0];
X=[X x];
r1=[r1; r];
a1=a1*(180/pi);
hold on
%plot(x,abs(fzero(@ (a) (2*a)+2*cos(x)*tan(x-a),i)), 'r+');
hold on
%plot(x,abs(F0), 'b^');
hold on
%end
F1
%var=[0.1:0.1:1;F'];
delta=delta*180/pi;
figure(2)
SUBPLOT(6,1,2),plot(i,delta,'b.','Linewidth',0.5);
hold on
SUBPLOT(6,1,3),plot(tan(a1),F0,'b.','Linewidth',0.5);
hold on

```

```

end
for i=0.3986:0.01:0.6486
    delta=-287*(pi/180);
    %for i=0.01:0.1:1
    x=delta/i_st;
    r=(U-(omega1_r*R_dyn*cos(x)))/(b/2); %determines the yaw rate of the vehicle
(rad/s)and lets assume the vehicle is making a left turn
    v= omega1_l*R_dyn*sin(x)-(a*r);% lateral velocity of the vehicle (m/s)
    %fzero(@(a) (2*Cf1*a)+m_v*omega1_l*R_dyn*cos(x)*tan(x-a),2000); %Evaluating
front tire slip angle, a (rad)
    %F0=-2*Cf1*fzero(@(a) (2*Cf1*a)+m_v*omega1_l*R_dyn*cos(x)*tan(x-a),2000);
%Evaluating the front left(inner) tire lateral force (N)
    %F2=[];
    a1=((v+a*r)/U)-x; %slip angle of the front wheel (rad)
    F0=-2*Cf1*a1;
    F2=[F2; F0];
    X=[X x];
    hold on
    r2=[r2; r];
    %plot(x,abs(fzero(@(a) (2*a)+2*cos(x)*tan(x-a),i)), 'r+');
    a1=a1*(180/pi);
    hold on
    %plot(x,abs(F0), 'b. ');
    %end
    F2
    %var=[0.1:0.1:21;F'];
    delta=delta*180/pi;
    figure(2)
    SUBPLOT(6,1,2),plot(i,delta,'b.', 'Linewidth',0.5);

```

```

hold on
SUBPLOT(6,1,3),plot(tan(a1),F0,'b.','Linewidth',0.5);
hold on
end
for i=0.6486:0.01:1.0472
    delta=((720*i)-753.992)*(pi/180);
    %for i=0.01:0.1:1
        x=delta/i_st;
        %fzero(@(a) (2*Cf1*a)+m_v*omega1_l*R_dyn*cos(x)*tan(x-a),2000);
%Evaluating front tire slip angle, a (rad)
        %F0=-2*Cf1*fzero(@(a) (2*Cf1*a)+m_v*omega1_l*R_dyn*cos(x)*tan(x-
a),2000); %Evaluating the front left(inner) tire lateral force (N)
        r=((omega1_r*R_dyn*cos(x))-U)/(b/2); %determines the yaw rate of the vehicle
(rad/s)
        v=(omega1_l*R_dyn*sin(x))-(a*r);% lateral velocity of the vehicle (m/s)
        %F3=[];
        a1=((v+a*r)/U)-x; %slip angle of the front wheel (rad)
        F0=-2*Cf1*a1;
        F3=[F3; F0];
        X=[X x];
        hold on
        r3=[r3; r];
        %plot(x,abs(fzero(@(a) (2*a)+2*cos(x)*tan(x-a),i)), 'r+');
        a1=a1*(180/pi);
        hold on
        %plot(x,abs(F0), 'b. ');
        hold on
%end
F3

```

```

%var=[0.1:0.1:21;F'];
delta=delta*180/pi;
figure(2)
SUBPLOT(6,1,2),plot(i,delta,'b.','Linewidth',0.5);
hold on
SUBPLOT(6,1,3),plot(tan(a1),F0,'b.','Linewidth',0.5);
hold on
end
for i=1.0472:0.01:1.4458
    delta=((720*i)-753.992)*(pi/180);
    %for i=0.01:0.1:1
        x=delta/i_st;
        %fzero(@a)          (2*Cf1*a)+m_v*omega1_1*R_dyn*cos(x)*tan(x-a),2000);
%Evaluating front tire slip angle, a (rad)
        %F0=-2*Cf1*fzero(@a)          (2*Cf1*a)+m_v*omega1_1*R_dyn*cos(x)*tan(x-
a),2000); %Evaluating the front left(inner) tire lateral force (N)
        r=(U-(omega1_1*R_dyn*cos(x)))/(b/2); %determines the yaw rate of the vehicle
(rad/s)
        v=(omega1_1*R_dyn*sin(x))-(a*r);% lateral velocity of the vehicle (m/s)
        %F3=[];
        a1=((v+a*r)/U)-x; %slip angle of the front wheel (rad)
        F0=-2*Cf1*a1;
        F4=[F4; F0];
        X=[X x];
        hold on
        r4=[r4; r];
        %plot(x,abs(fzero(@a) (2*a)+2*cos(x)*tan(x-a),i)), 'r+');
        a1=a1*(180/pi);
        hold on

```



```

    %plot(x,abs(F0),'b.');
```

hold on

```

%end
F4
%var=[0.1:0.1:21;F'];
delta=delta*180/pi;
figure(2)
SUBPLOT(6,1,2),plot(i,delta,'b.','Linewidth',0.5);
hold on
SUBPLOT(6,1,3),plot(tan(a1),F0,'b.','Linewidth',0.5);
hold on
end
for i=1.4458:0.01:4.4458
    delta=287*(pi/180);
    %for i=0.01:0.1:1
        x=delta/i_st;
        %fzero(@a)          (2*Cf1*a)+m_v*omega1_l*R_dyn*cos(x)*tan(x-a),2000);
%Evaluating front tire slip angle, a (rad)
        %F0=-2*Cf1*fzero(@a)          (2*Cf1*a)+m_v*omega1_l*R_dyn*cos(x)*tan(x-
a),2000); %Evaluating the front left(inner) tire lateral force (N)
        r=(U-(omega1_l*R_dyn*cos(x)))/(b/2); %determines the yaw rate of the vehicle
(rad/s)
        v=(omega1_r*R_dyn*sin(x)-(a*r));% lateral velocity of the vehicle (m/s)
        %F3=[];
        a1=((v+a*r)/U)-x; %slip angle of the front wheel (rad)
        F0=-2*Cf1*a1;
        F5=[F5; F0];
        X=[X x];
        a1=a1*(180/pi);

```

```

hold on
r5=[r5; r];
%plot(x,abs(fzero(@(a) (2*a)+2*cos(x)*tan(x-a),i)), 'r+');
hold on
%plot(x,abs(F0), 'b. ');
hold on
%end
F5
%var=[0.1:0.1:21;F'];
delta=delta*180/pi;
figure(2)
SUBPLOT(6,1,2),plot(i,delta, 'b.', 'Linewidth',0.5);
hold on
SUBPLOT(6,1,3),plot(tan(a1),F0, 'b.', 'Linewidth',0.5);
hold on
end
for i=4.4458:0.01:6.4458
delta=(287-143.5*(i-4.4458))*(pi/180);
%for i=0.01:0.1:1
x=delta/i_st;
r=((omega1_l*R_dyn*cos(x))-U)/(b/2); %determines the yaw rate of the vehicle
(rad/s)
v= omega1_l*R_dyn*sin(x)-(a*r);% lateral velocity of the vehicle (m/s)
%fzero(@(a) (2*Cf1*a)+m_v*omega1_l*R_dyn*cos(x)*tan(x-a),2000);
%Evaluating front tire slip angle, a (rad)
%F0=-2*Cf1*fzero(@(a) (2*Cf1*a)+m_v*omega1_l*R_dyn*cos(x)*tan(x-
a),2000); %Evaluating the front left(inner) tire lateral force (N)
%F4=[];
a1=((v+a*r)/U)-x; %slip angle of the front wheel (rad)

```

```

F0=-2*Cf1*a1;
F6=[F6; F0];
X=[X x];
a1=a1*(180/pi);
hold on
r6=[r6; r];
%plot(x,abs(fzero(@(a) (2*a)+2*cos(x)*tan(x-a),i)), 'r+');
hold on
%plot(x,abs(F0), 'b. ');
hold on
%end
F6
delta=delta*180/pi;
figure(2)
SUBPLOT(6,1,2),plot(i,delta,'b.', 'Linewidth',0.5);
hold on
SUBPLOT(6,1,3),plot(tan(a1),F0,'b.', 'Linewidth',0.5);
hold on
end
r_var=[r1;r2;r3;r4;r5;r6];
r_var1=[1/100:1/100:648/100;r_var'];
hold on
var=[F1;F2;F3;F4;F5;F6];
var1=[1/100:1/100:648/100;var'];
figure(1)
plot(1/100:1/100:648/100,r_var1(2,:))
save yaw_rate.mat
clear r1 r2 r3 r4 r5 r6 r_var r_var1 r V_speed g h_o
clear Cf1 R1 R_i V V_i X b i omega1_l omega_sys F0 R_dyn R_o V_final V_o

```

```

clear ans delta i_st omega1_r x E R t F F1 F2 F3 F4 F5 F6 var m_v a b a1 Tw1 v U
who %declares variables in the current workspace
figure(2)
SUBPLOT(6,1,1), plot(1/100:1/100:648/100,var1(2,:))
hold on
who
save today_hari.mat %saves the workspace into a *.mat file
DLMWRITE('data.txt',var1(2:),'newline','pc')
%-----
% The first half of the code calculates the tire forces for a left tire as
% it makes a right turn (when it becomes the outer tire) and left turn (when
% it becomes the inner tire)
clc
clear all
syms x
Cf1=7.0*10e4; %Front tire cornering stiffness (N/rad)
R_dyn=0.3; %Dynamic Tire Radius(m)
i_st=15; %Steering system gear ratio
% According to DOT, for a speed of 64.5 mph, the radius of the horizontal
% curve is about 2500 feet. Hence a speed of 71mph, 10% more than the safe
% limit is assumed.
%R=2500; % Units are in feet
%E=0; % Superelevation is assumed to be zero
%V=((-0.03*R)+((0.03*R)^2+4*R*(15*(E/100)+3.6))^0.5)/2; % Units are in mph
V_speed=50;%units are in mph
V_final=50*0.44704; %units converted into m/s
%V_final=1.10*V
%omega_tires=(V_final/(R_dyn) %Speed is converted from mph to m/s and radius is
converted from feet to meters. Units are rad/s.

```

```

%Breadth of vehicle=b
m_v=2000;
%R1=R*0.3048; %Units are in meters
a=1.4; %distance c.g to front axle
b=1.50; %track width of the vehicle
%h_o=0.183 %height of the vehicle C.G above the ground
%g = 9.81 %acceleration due to gravity in m/s2
%R=((V_final*V_final)*2*h_o)/(0.8*g*b); %here it is assumed that the fishhook
maneuver turns to 287 degrees with +sign for a right turn
%omega_sys=V_final/R;
%R_i=R-(b/2); %assuming no vehicle body side slip angle
%V_i=R_i*omega_sys;
%R_o=R+(b/2);
%V_o=R_o*omega_sys;
omega1_l=V_final/R_dyn;
omega1_r=V_final/R_dyn;
U=V_final; %Forward speed of the vehicle in m/s
%Tw1=1.5; %track width of the vehicle
F=[];
F1=[];
F2=[];
F3=[];
F4=[];
F5=[];
F6=[];
X=[];
r1=[];
r2=[];
r3=[];

```

```

r4=[];
r5=[];
r6=[];
for i=0:0.01:0.3986
    delta=(720*i)*(pi/180);
    x=delta/i_st;
    r=((omega1_l*R_dyn*cos(x))-U)/(b/2); %determines the yaw rate of the vehicle
(rad/s)
    v=(omega1_l*R_dyn*sin(x))-(a*r);% lateral velocity of the vehicle (m/s)
    %fzero(@a (2*Cf1*a)+m_v*omega1_l*R_dyn*cos(x)*tan(x-a),2000); %Evaluating
front tire slip angle, a (rad)
    %F0=-2*Cf1*fzero(@a (2*Cf1*a)+m_v*omega1_l*R_dyn*cos(x)*tan(x-a),2000);
%Evaluating the front left(inner) tire lateral force (N)
    a1=((v+a*r)/U)-x; %slip angle of the front wheel (rad)
    F0=-2*Cf1*a1;
    F1=[F1; F0];
    X=[X x];
    r1=[r1; r];
    a1=a1*(180/pi);
    hold on
    %plot(x,abs(fzero(@a (2*a)+2*cos(x)*tan(x-a),i)), 'r+');
    hold on
    %plot(x,abs(F0), 'b^');
    hold on
    %end
    F1
    %var=[0.1:0.1:1;F'];
    delta=delta*180/pi;
    figure(2)

```

```

SUBPLOT(6,1,4),plot(i,delta,'k.','Linewidth',0.5);
hold on
SUBPLOT(6,1,5),plot(tan(a1),F0,'k.','Linewidth',0.5);
hold on
end
for i=0.3986:0.01:0.6486
    delta=-287*(pi/180);
    %for i=0.01:0.1:1
    x=delta/i_st;
    r=((omega1_1*R_dyn*cos(x))-U)/(b/2); %determines the yaw rate of the vehicle
(rad/s)and lets assume the vehicle is making a left turn
    v= omega1_1*R_dyn*sin(x)-(a*r);% lateral velocity of the vehicle (m/s)
    %fzero(@(a) (2*Cf1*a)+m_v*omega1_1*R_dyn*cos(x)*tan(x-a),2000); %Evaluating
front tire slip angle, a (rad)
    %F0=-2*Cf1*fzero(@(a) (2*Cf1*a)+m_v*omega1_1*R_dyn*cos(x)*tan(x-a),2000);
%Evaluating the front left(inner) tire lateral force (N)
    %F2=[];
    a1=((v+a*r)/U)-x; %slip angle of the front wheel (rad)
    F0=-2*Cf1*a1;
    F2=[F2; F0];
    X=[X x];
    hold on
    r2=[r2; r];
    %plot(x,abs(fzero(@(a) (2*a)+2*cos(x)*tan(x-a),i)), 'r+');
    a1=a1*(180/pi);
    hold on
    %plot(x,abs(F0), 'b. ');
%end
F2

```

```

% var=[0.1:0.1:21;F'];
delta=delta*180/pi;
figure(2)
SUBPLOT(6,1,4),plot(i,delta,'k.','Linewidth',0.5);
hold on
SUBPLOT(6,1,5),plot(tan(a1),F0,'k.','Linewidth',0.5);
hold on
end
for i=0.6486:0.01:1.0472
    delta=((720*i)-753.992)*(pi/180);
    %for i=0.01:0.1:1
        x=delta/i_st;
        %fzero(@(a) (2*Cf1*a)+m_v*omega1_1*R_dyn*cos(x)*tan(x-a),2000);
%Evaluating front tire slip angle, a (rad)
        %F0=-2*Cf1*fzero(@(a) (2*Cf1*a)+m_v*omega1_1*R_dyn*cos(x)*tan(x-
a),2000); %Evaluating the front left(inner) tire lateral force (N)
        r=(U-(omega1_1*R_dyn*cos(x)))/(b/2); %determines the yaw rate of the vehicle
(rad/s)
        v=(omega1_1*R_dyn*sin(x)-(a*r));% lateral velocity of the vehicle (m/s)
        %F3=[];
        a1=((v+a*r)/U)-x; %slip angle of the front wheel (rad)
        F0=-2*Cf1*a1;
        F3=[F3; F0];
        X=[X x];
        hold on
        r3=[r3; r];
        %plot(x,abs(fzero(@(a) (2*a)+2*cos(x)*tan(x-a),i)), 'r+');
        a1=a1*(180/pi);
        hold on

```



```

    %plot(x,abs(F0),'b.');
```

hold on

```

%end
F3
%var=[0.1:0.1:21;F'];
delta=delta*180/pi;
figure(2)
SUBPLOT(6,1,4),plot(i,delta,'k.','Linewidth',0.5);
hold on
SUBPLOT(6,1,5),plot(tan(a1),F0,'k.','Linewidth',0.5);
hold on
end
for i=1.0472:0.01:1.4458
    delta=((720*i)-753.992)*(pi/180);
    %for i=0.01:0.1:1
        x=delta/i_st;
        %fzero(@a)          (2*Cf1*a)+m_v*omega1_l*R_dyn*cos(x)*tan(x-a),2000);
%Evaluating front tire slip angle, a (rad)
        %F0=-2*Cf1*fzero(@a)      (2*Cf1*a)+m_v*omega1_l*R_dyn*cos(x)*tan(x-
a),2000); %Evaluating the front left(inner) tire lateral force (N)
        r=((omega1_r*R_dyn*cos(x))-U)/(b/2); %determines the yaw rate of the vehicle
(rad/s)
        v=(omega1_l*R_dyn*sin(x))-(a*r);% lateral velocity of the vehicle (m/s)
        %F3=[];
        a1=((v+a*r)/U)-x; %slip angle of the front wheel (rad)
        F0=-2*Cf1*a1;
        F4=[F4; F0];
        X=[X x];
        hold on

```

```

r4=[r4; r];
%plot(x,abs(fzero(@(a) (2*a)+2*cos(x)*tan(x-a),i)), 'r+');
a1=a1*(180/pi);
hold on
%plot(x,abs(F0), 'b. ');
hold on
%end
F4
%var=[0.1:0.1:21;F'];
delta=delta*180/pi;
figure(2)
SUBPLOT(6,1,4),plot(i,delta,'k.', 'Linewidth',0.5);
hold on
SUBPLOT(6,1,5),plot(tan(a1),F0,'k.', 'Linewidth',0.5);
hold on
end
for i=1.4458:0.01:4.4458
    delta=287*(pi/180);
    %for i=0.01:0.1:1
        x=delta/i_st;
        %fzero(@(a) (2*Cf1*a)+m_v*omega1_l*R_dyn*cos(x)*tan(x-a),2000);
%Evaluating front tire slip angle, a (rad)
        %F0=-2*Cf1*fzero(@(a) (2*Cf1*a)+m_v*omega1_l*R_dyn*cos(x)*tan(x-
a),2000); %Evaluating the front left(inner) tire lateral force (N)
        r=((omega1_r*R_dyn*cos(x))-U)/(b/2); %determines the yaw rate of the vehicle
(rad/s)
        v=(omega1_r*R_dyn*sin(x)-(a*r));% lateral velocity of the vehicle (m/s)
        %F3=[];
        a1=((v+a*r)/U)-x; %slip angle of the front wheel (rad)

```

```

F0=-2*Cf1*a1;
F5=[F5; F0];
X=[X x];
a1=a1*(180/pi);
hold on
r5=[r5; r];
%plot(x,abs(fzero(@(a) (2*a)+2*cos(x)*tan(x-a),i)), 'r+');
hold on
%plot(x,abs(F0), 'b. ');
hold on
%end
F5
%var=[0.1:0.1:21;F'];
delta=delta*180/pi;
figure(2)
SUBPLOT(6,1,4),plot(i,delta,'k.', 'Linewidth',0.5);
hold on
SUBPLOT(6,1,5),plot(tan(a1),F0,'k.', 'Linewidth',0.5);
hold on
end
for i=4.4458:0.01:6.4458
    delta=(287-143.5*(i-4.4458))*(pi/180);
    %for i=0.01:0.1:1
        x=delta/i_st;
        r=(U-(omega1_r*R_dyn*cos(x)))/(b/2); %determines the yaw rate of the vehicle
(rad/s)
        v= omega1_l*R_dyn*sin(x)-(a*r);% lateral velocity of the vehicle (m/s)
        %fzero(@(a) (2*Cf1*a)+m_v*omega1_l*R_dyn*cos(x)*tan(x-a),2000);
%Evaluating front tire slip angle, a (rad)

```

```

    %F0=-2*Cf1*fzero(@a)      (2*Cf1*a)+m_v*omega1_l*R_dyn*cos(x)*tan(x-
a),2000); %Evaluating the front left(inner) tire lateral force (N)
    %F4=[];
    a1=((v+a*r)/U)-x; %slip angle of the front wheel (rad)
    F0=-2*Cf1*a1;
    F6=[F6; F0];
    X=[X x];
    a1=a1*(180/pi);
    hold on
    r6=[r6; r];
    %plot(x,abs(fzero(@a) (2*a)+2*cos(x)*tan(x-a),i),'r+');
    hold on
    %plot(x,abs(F0),'b.');
```

```

    hold on
%end
F6
delta=delta*180/pi;
figure(2)
SUBPLOT(6,1,4),plot(i,delta,'k.','Linewidth',0.5);
hold on
SUBPLOT(6,1,5),plot(tan(a1),F0,'k.','Linewidth',0.5);
hold on
end
r_var_r=[r1;r2;r3;r4;r5;r6];
r_var1_r=[1/100:1/100:648/100;r_var_r'];
hold on
var_r=[F1;F2;F3;F4;F5;F6];
var1_r=[1/100:1/100:648/100;var_r'];
figure(3)

```

```

plot(1/100:1/100:648/100,r_var1_r(2,:))
save yaw_rate_r.mat
clear r1 r2 r3 r4 r5 r6 r_var_r r_var1_r r V_speed g h_o
clear Cf1 R1 R_i V V_i X b i omega1_l omega_sys F0 R_dyn R_o V_final V_o
clear ans delta i_st omega1_r x E R t F F1 F2 F3 F4 F5 F6 var_r m_v a b a1 Tw1 v U
who %declares variables in the current workspace
figure(2)
SUBPLOT(6,1,6), plot(1/100:1/100:648/100,var1_r(2,:))
hold on
who
save today_hari_r.mat %saves the workspace into a *.mat file
sim('hac_model_simulink') %runs the simulation model in simulink
figure
%plot(X,F)
DLMWRITE('data_r.txt',var1_r(2,:),'newline','pc')
% Regression Analysis to estimate accurate roll angles
W_s=(700*9.81); %N
h2=0.560; %m
g=9.81; %m/s2
y0=0.1; %m
I_o=8400000;
k_phi=3.2230e+003; %N-m/rad
x=simout';
phi=((W_s*x*h2/g)+(W_s*y0))/(k_phi-(W_s*h2));% steady state roll angle
p=polyfit(x,phi,1);
f = polyval(p,x);
figure(3)
plot(x,phi,'o',x,f,'-')
%axis([-3 3 -2 2])

```

```

p
beta=p(:,1);
alpha=p(:,2);
h2_m=(alpha*k_phi)/((W_s/g)*(1+g*alpha));
y0_m=beta*(k_phi-((W_s/g)*g*h2_m))/W_s;
I=I_o+(W_s/g)*(h2^2+(y0_m)^2);
phi_st0=(W_s*y0)/(k_phi-(W_s*h2));
phi_n=((W_s*x*h2_m/g)+(W_s*y0_m))/(k_phi-(W_s*h2_m));
phi_sd=phi_n-phi_st0;
figure(4)
plot(x,phi_sd)
plot(simout',phi_sd)
plot(simout', phi_n)
plot(1/100:1/100:1962/100,phi_n)
hold on
plot(1/100:1/100:1962/100,phi)
anova1(phi_n'-phi');
%LTR for the trailer
LTR= (simout2-simout1)/ (W_s/2);

```

APPENDIX-III

VEHICLE PARAMETERS USED FOR STUDY

<i>Sprung Mass</i>	$m_{sprung} = 350 \text{ kg}$
<i>Unsprung Mass</i>	$m_{unsprung} = 31 \text{ kg}$
<i>Damping constant of the Spring</i>	$c_{damping} = 1140 \text{ N/m/s}$
<i>Stiffness of the suspension system</i>	$k_{suspension} = 20\,900 \text{ N/m}$
<i>Tire Stiffness</i>	$k_{tires} = 10800 \text{ N/m}$
<i>Front Tire Cornering Stiffness</i>	$C_{Fa1} = 7.0 \times 10^4 \text{ N/rad}$
<i>Dynamic Tire Radius</i>	$R_{dyn} = 0.3 \text{ m}$
<i>Steering Gear ratio</i>	$i_{st} = 15$
<i>Entry Speed</i>	$U = 50 \text{ mph}$
<i>Distance from C.G to front axle</i>	$a = 1.4 \text{ m}$
<i>Track Width of the Vehicle</i>	$b = 1.50 \text{ m}$
<i>Acceleration due to gravity</i>	$g = 9.81 \text{ m/s}^2$
<i>Stiffness of tire</i>	$k_{tires} = 10\,800 \text{ N/m}$

APPENDIX IV

DERIVATION OF ROLL ANGLE DETERMINATION FOR SUSPENSION RELATIVE POSITION SENSOR MEASUREMENT

In a suspension system, the tire roll stiffness and the suspension roll stiffness can be modeled as torsion springs in series.

For Torsion Springs in series (with unequal stiffnesses):

The moment is same, but the angle of twist is different

For Torsion Springs in parallel (with unequal stiffnesses):

The moment is different, but the angle of twist is the same.

Since for torsion springs in series, the moment acting on the two springs are same, due to the variation in torsional stiffness, the springs would twist by different angles.

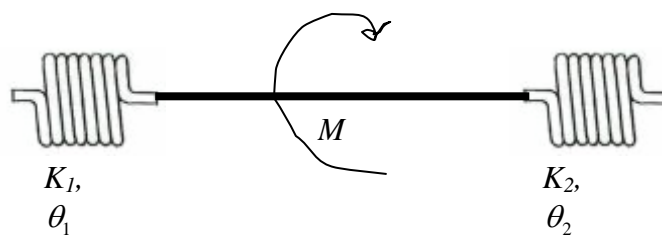


Fig. 1-A Two springs in series subjected to moment, M

The total stiffness is given by the Equation 1-A,

$$\frac{1}{K} = \frac{1}{k_1} + \frac{1}{k_2} \Rightarrow \frac{1}{K_{totalrollstiffness}} = \frac{1}{k_{tire}} + \frac{1}{k_{suspension}} \quad 1-A$$

For a torsional spring, the relation connecting the twist angle and the moment is given by Equation 2-A,

$$\phi = k.M \quad 2-A$$

Where ϕ = roll/ twist angle (rad)

k = tire compliance ($rad.N^{-1}.m^{-1}$) = reciprocal of tire stiffness

M = moment (N/m)

Therefore substituting Equation 2-A in Equation 1-A, Equation 3-A results as

$$\frac{\phi_{total}}{M_{totalmoment}} = \frac{\phi_{tire(axleroll)}}{M_{totalmoment}} + \frac{\phi_{suspension}}{M_{totalmoment}} \Rightarrow \phi_{total} = \phi_{tire(axleroll)} + \phi_{suspension} \quad 3-A$$

Therefore, the total roll angle due is given by the following Equation 4-A.

$$\phi_{total} = \phi_{sus} + \phi_{tire(axleroll)} \quad 4-A$$

The roll angle due to tire roll moment is given by Equation 5-A

$$\phi_{tire(axleroll)} = \frac{Total\ Roll\ Moment}{Tire\ Roll\ Stiffness} = Total\ Roll\ Moment \times Tire\ Roll\ Compliance$$

$$\phi_{tire(axleroll)} = \frac{Ma_y h}{k_{tire}} \quad 5-A$$

And the roll angle due to suspension movement is given by Equations 6-A.

$$\phi_{sus} = \frac{\Delta z_{i,j}}{t_w} \quad 6-A$$

Where $\Delta z_{i,j}$ = average suspension deflections at the left and right side of the vehicle

t_w = track width of the vehicle

Therefore, substituting Equations 5-A and 6-A in Equation 4-A results in Equation 7-A,

$$\phi_{total} = \frac{\Delta z_{i,j}}{t_w} - \frac{Ma_y h}{k_{tire}} \quad 7-A$$

VITA

Narahari Vittal Rao graduated with a Bachelors' Degree in mechanical engineering from R V College of Engineering affiliated to Vishveswariah Technological University in June 2002. Later on he went on to work for Toyota Motor Corporation, India as an engineer in the Product Design and Development Division. Having worked on the Indian Corolla and Innova Projects, in the fall of 2003, he joined Texas A&M University to begin his Masters' in mechanical engineering.

His research interests primarily include vehicle dynamics, testing and evaluation procedures and also race car technology. His permanent address is #22/1, Margosa Road, 3rd Main, Malleswaram, Bangalore- 560 003, Karnataka, India. His e-mail id is narahari_v@hotmail.com.